CHALMERS
UNIVERSITY OF TECHNOLOGY

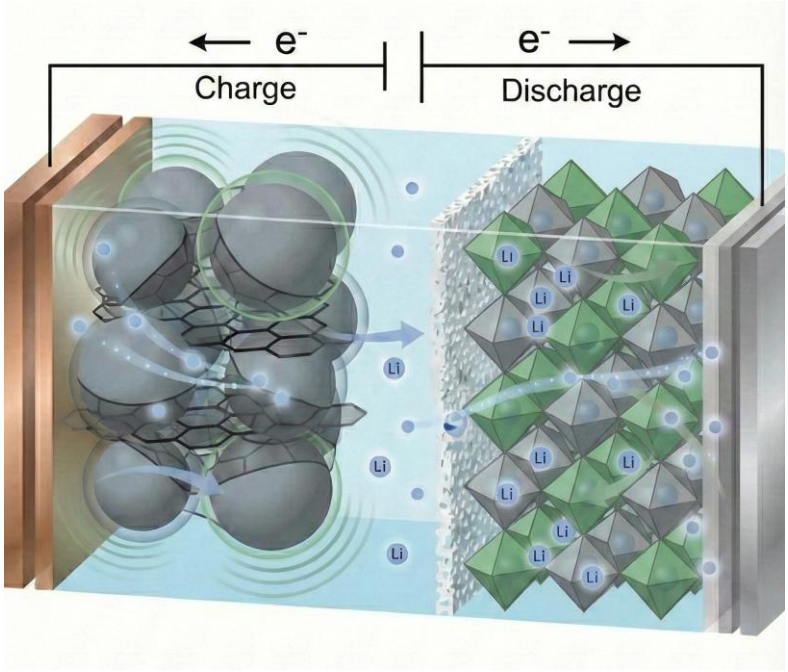

Enhancing the Lithium-Ion Battery Performance of Commercial Micron-sized Silicon Particles using Graphene

Master's thesis in
Industrial and Materials Science

Preeth Namagondlu Kishan

DEPARTMENT OF INDUSTRIAL AND MATERIALS SCIENCE

CHALMERS UNIVERSITY OF TECHNOLOGY
Gothenburg, Sweden 2026
www.chalmers.se

MASTER'S THESIS IN SUSTAINABLE ENERGY SYSTEMS

Enhancing the Lithium-Ion Battery Performance of Commercial Micron-sized Silicon Particles using Graphene

CHALMERS
UNIVERSITY OF TECHNOLOGY

PREETH NAMAGONDLU KISHAN

Department of Industrial and Materials Science
Division of Sustainable Energy Systems
CHALMERS UNIVERSITY OF TECHNOLOGY
Göteborg, Sweden 2026

Enhancing the Lithium-Ion Battery Performance of Commercial Micron-sized Silicon Particles using Graphene

PREETH NAMAGONDLU KISHAN

Supervisor: Dr. Nitish Kumar, Industrial and Materials Science
Examiner: Dr. Jinhua Sun, Industrial and Materials Science

Department of Industrial and Materials Science
Division of Sustainable Energy Systems
Chalmers University of Technology
SE-412 96 Göteborg
Sweden
Telephone: + 46 (0)31-772 1000

Enhancing the Lithium-Ion Battery Performance of Commercial Micron-sized Silicon Particles using Graphene
Master’s thesis in Master’s programme Sustainable Energy Systems
PREETH NAMAGONDLU KISHAN
Department of Industrial and Materials Science
Division of Sustainable Energy Systems
Chalmers University of Technology

Abstract

Silicon is known to be one of the most promising anode material for future-generation lithium-ion batteries, thanks to its theoretical specific capacity of approximately 3579 mAh/g. Nonetheless, the use of silicon anodes is hampered in practical devices owing to their large volume expansion during lithiation, the instability of the solid electrolyte interface, capacity decay, and poor rechargeability. Specifically, micron-sized commercial-grade silicon particles exhibit drastic pulverization, along with the loss of electrical contact, during the cycling process. This thesis attempts to improve the electrochemical properties of commercial micron-sized silicon materials by thick graphene coating. A comprehensive strategy included the size reduction of the materials via ball mill processing, the introduction of functional groups through APTES silanization, the deposition of graphene oxide, and finally, chemical reduction of the resultant material on the surface of the silicon materials to create a graphene layer. The optimized ball-milled, uniformly graphene-coated silicon electrodes revealed a remarkably high discharge capacity of about 3400 $mAhg^{-1}$. Significantly improved stability was also observed, retaining a discharge capacity of 1600-1800 $mAhg^{-1}$ after 25 cycles in a designed half-cell. However, the unmodified silicon electrodes, along with the non-uniformly modified samples, suffered from a sharp decrease in discharge capacities below the 500 $mAhg^{-1}$mark. These findings prove the effectiveness of homogeneous graphitic coatings, together with size reduction, in reducing the volume expansion of silicon and preserving electrical connections. This work presents a feasible, affordable method to enhance the performance of commercial, micron-sized Si anode materials, filling the technological gap between the lab scale and commercial Li-ion batteries (LIB).

Key words:

Lithium-ion batteries; Silicon anode; Graphene; Uniform Coating; Scalable electrode fabrication;

List of Acronyms

APTES	(3-Aminopropyl)triethoxysilane
CE	Coulombic Efficiency
CV	Cyclic Voltammetry
DI	Deionized
EIS	Electrochemical Impedance Spectroscopy
GO	Graphene Oxide
GCD	Galvanostatic Charge–Discharge
ICE	Initial Coulombic Efficiency
LIB	Lithium-Ion Battery
PVDF	Poly(vinylidene fluoride)
rGO	Reduced Graphene Oxide
R_{ct}	Charge-Transfer Resistance
R_s	Solution (Electrolyte) Resistance
SEI	Solid Electrolyte Interphase
SEM	Scanning Electron Microscopy
Si	Silicon
Si@rGO	Graphene-coated silicon
wt%	Weight percentage
XRD	X-ray Diffraction

Notations

C	Specific discharge capacity	mAh g^{-1}
C_0	Initial discharge capacity	mAh g^{-1}
C_n	Discharge capacity at cycle (n)	mAh g^{-1}
CR	Capacity retention	%
E	Cell potential	V
I	Current	A
i	Current density	mA g^{-1}
n	Cycle number	—
R	Electrical resistance	Ω
R_{ct}	Charge-transfer resistance (EIS semicircle)	Ω
R_s	Electrolyte resistance	Ω
Z'	Real part of impedance	Ω
-Z"	Imaginary part of impedance	Ω

Contents

List of Figures

List of Tables

Preface

This thesis has been conducted in connection with the Master's programme in Industrial and Materials Science at Chalmers University of Technology. This has been done during the spring term of 2025. This project is an endeavor to improve the electrochemical properties of micron-sized silicon particles for anode materials in lithium-ion batteries using surface modification with graphene.

The research in this thesis focuses on the key issues in the use of silicon anodes, including volume expansion, interfacial instability, and capacity decay during cycling. By modifying particle size, surface functionalization, optimizing graphene coating, and performing electrochemical analysis, the proposed thesis will advance the stable use of the silicon anode material. The experimental analysis of the new material is associated with electrochemical cycling measurement, including cyclic galvanostatic charge–discharge, cyclic voltammetry, electrochemical impedance and others. During the course of this project, I have learned a lot about designing experiments, characterizing materials, and analyzing results, and I have developed an appreciation for the connection between the structure of materials and their electrochemical properties. This project represents my growing academic interest in energy storage materials.

The research work took place in the department of Mechanics and Maritime Sciences at the Chalmers University of Technology, which provided a conducive environment and resources necessary for the success of the thesis work.

Acknowledgements

I would like to thank Dr. Nitish Kumar, a Postdoctoral researcher, for his valuable guidance and encouragement throughout this thesis. His knowledge and contributions to this field proved invaluable to me and played an important role in shaping my experiential process for this study.

I would like to express my gratitude to my examiner, Dr. Jinhua Sun, from the Department of Industrial and Materials Sciences, for his valuable feedback, thoughtful suggestions, and critical assessment of this research. His contribution is highly appreciated, which has added much to the scientific aspects presented in this thesis.

I would like to thank my fellow students and colleagues for their cooperation, discussions, and sharing experiences in the course of this project. I am very grateful for the technical support in the laboratory, which allowed the experimental work to be done smoothly and without disruption.

Finally, I would like to extend my heart's gratitude to my family and friends for their never-ceasing encouragement, patience, and support throughout the period in which I have been at this university. Their understanding and faith in my capabilities have been a constant source of motivation in the completion of this thesis.

Göteborg March 2026-02-04

PREETH NAMAGONDLU KISHAN

1 Introduction

Lithium-ion batteries (LIBs) have become the basis of modern energy storage due to their usage in electric vehicles, portable electronics, and renewable energy systems. Part of the reason for their popularity is the existing manufacturing technologies, long storage and cycle life, and energy density. However, current LIB technology has an unresolved issue with the anode. Their performance and energy density still rely on the anode, which is constrained to 372 mAh g^{-1}. Advanced applications like EVs with long-range drives and large storage grids will continue to not meet demand (1). Owing to its theoretical specific capacity of ~3579 mAh g^{-1} (for $Li_{15}Si_4$), silicon is one of the most appealing substitutes for graphite. Apart from deployment and ecological consideration, silicon is also one of the materials that could tremendously enhance the volumetric and gravimetric energy density of LIBs (2). Enhanced performance in stationary batteries, EVs with longer driving ranges, and portable devices with reduced battery mass could be achieved by unlocking the full potential of silicon in commercial energy systems.

While there are many conveniences attributed to using silicon as anode material, there are equally significant challenges present. The most important challenge is during lithiational process where mechanical stress is generated. The mechanical stress during lithiation causes the silicon to volumetrically expand up to an outrageously large 300% (3). In addition to the mechanical stress including compressive, tensile, shear, and interfacial stresses arising from repeated lithiation-induced volume expansion the silicon is easily expanded, and therefore, physical and electrical disconnections can occur, which will lead to decreased performance during cycling. In addition, silicon is not as conductive as graphite, which inhibits the electrochemical reaction from fully developing (4). The easily brittle silicon particles lose cohesion due to weak SEI, causing the interphase to continuously and rapidly degrade (5).

A great deal of research has been done on various silicon nanostructures (such as nanoparticles, nanowires, and porous silicon) with the intent of resolving the problems associated with silicon anodes. Decreasing the size of the particles tends to increase the ability of a structure to withstand mechanical stress and reduces the lengths to which lithium must diffuse. That being said, the issues with nano-silicon include high costs, complex and difficult to scale synthesis, low practicality for industrial use and high surface area which excessive solid electrolyte interface (SEI) formation or substantial irreversible capacity losses. (6) Micron-sized silicon particles, on the other hand, can provide significant industrial value because they are relatively low in cost, readily available (for instance, from waste products created when cutting silicon wafers), and have a higher tap density than nano-silicon. The ability to achieve a high volumetric energy density (which is essential for electric vehicle and stationary use) at low cost is of immense value. This said, silicon particles in the micron range are more susceptible to mechanical degradation and cracking because they are larger in size thus there is a critical need for more effective structural engineering techniques which can stabilize micron size silicon particles without sacrificing low cost and high scalability (7).

Among the many explored strategies, the use of graphene is the most successful material for improving the electrochemical properties of silicon anodes. Graphene is a 2d material made of sp2-hybridized carbon atoms. It has excellent electrical, mechanical, and physical properties, including large surface area and flexibility. For this reason, it is well suited for addressing the challenges of silicon based anodes. More

specifically, graphene has multiple synergistic effects when incorporated with micron sized silicon: it acts as an ultrathin highly conductive grid that enhances charge transport, it is highly flexible and provides mechanical buffering to the silicon's large volume expansion, it's conformal coating on silicon surfaces inhibits direct electrolyte exposure and stabilizes the SEI, and it provides stable electrodes with high areal capacities (8). New research results indicate progress in the field of graphene-sillicon composites. Wrinkled multilayer graphene coatings on commercial silicon microparticles showed improvement in cycle life and greater areal capacity (6). Reduced graphene oxide (rGO) frameworks that encapsulate silicon microparticles have been shown to enhance rate performance with added structural integrity (9). Low-cost, scalable methods like coal-derived graphene foams have shown in combination with micron-sized silicon to improve cycling stability in such systems, demonstrating their industrial potential (10). These results indicate that silicon's mechanical and electrochemical issues are no longer barriers due to the addition of graphene, which also moves silicon anodes closer to commercial use.

As said, there are still barriers to advancing practical graphene-silicon composites to be used in LIBs. The large-scale production of high quality or pristine graphene composites, along with the ability to uniformly coat silicon microparticles, still presents issues. The optimum balances of graphene encapsulation, porosity, electrode density, cycle life, capacity, and energy density are still not exactly known. The graphene synergistic effects coatings with electrolyte additives and binder systems also have not been fully studied (1). These issues in research are still crucial to the practicality of the use of graphene micron silicon composites. The capacity of silicon can provide LIB technology with a new direction, but these potential advancements are constrained by issues such as the mechanical, electrical, and interfacial properties. Combining micron-sized silicon with graphene creates a scientifically interesting and industrially practical avenue to explore. With the multifunctional role of graphene as a conductive network, mechanical buffer, and SEI stabilizer, it is ideally positioned to address the problems of silicon microparticles graphene silicon anodes. This thesis focuses on commercially available micron-sized silicon particles enhanced with graphene to develop electrodes for lithium-ion batteries, emphasizing scale-up, structural design to maintain long-term stability, and an assessment of the design's electrochemical performance.

1.1 Aim and Objectives

This thesis will design a scalable method for coating commercial micron-sized silicon particles with graphene that optimally improves their performance as anode materials for lithium-ion batteries. To achieve this goal, the project aims to develop a surface-modification and coating method, determine the best ratio of graphene to silicon and slurry formulations, and evaluate electrochemical performance of the coated materials with galvanostatic charge and discharge cycles, cyclic voltammetry, and electrochemical impedance spectroscopy.

The main objectives are,

- To develop a suitable coating method for micron-sized silicon particles with graphene.
- To optimise the graphene-to-silicon particle ratio for homogeneous coating and enhanced electrochemical stability.

- To enhance the slurry formulation and uniformity for dependable electrode production and consistent performance.

- To assess the electrochemical performance of the fabricated electrodes by galvanostatic charge-discharge cycling, cyclic voltammetry (CV), and electrochemical impedance spectroscopy (EIS).

- To establish a correlation between coating morphology, interfacial properties, electrochemical behaviour, and cycle stability of silicon-based anodes.

1.2 Background

Lithium-ion batteries (LIBs) have increasingly become essential to the modern world and are recognized as the primary energy storage technology used across portable electronics and electric vehicles (EVs) as well as in grid storage technologies. Some reasons as to why these batteries are considered to be the most reliable option are their energy density, long cycle lives, low self-discharge, and ease of mass production (1). Since Sony introduced these batteries commercially in 1991, improving the performance of cathodes, anodes, and electrolytes has advanced tremendously. Despite these developments, the industry standard of a graphite anode has not shown any significant improvement in energy density and therefore remains a problem with its low theoretical capacity of 372 mAh g^{-1} (8).
There are increased demands for energy storage, particularly for EVs and renewable energy, which underscores the need for materials with increased anode energy density. Silicon (Si) is among the leading candidates to replace or partially replace graphite, owing to its theoretical specific capacity of ~3579 $mAhg^{-1}$for $Li_{15}Si_4$ which is extraordinarily high, its low lithiation potential which is similar to graphite, and its relatively abundant in nature (4). Along with its high gravimetric capacity, silicon has a remarkable volumetric capacity of ~2190 mAh cm^{-3}, which is particularly valuable for electric vehicles (5).

The use of silicon for commercial and industrial purposes already has its drawbacks, to begin with, it undergoes lithiation, which causes it to undergo volumetric expansion for around 300%. The expansion and contraction of silicon whenever it undergoes lithiation, causes it to undergo mechanical stress, particle pulverization, rapid capacity fading, and electric isolation (3). Moreover, its conductivity, which is around 0.00001 S/cm, severely limits silicon's rate capability. The further solid-electrolyte interphase increases these issues. Lithium is lost along with a decrease in cycle life because of cracked silicon particles, and newly exposed surfaces that undergo reactions with the electrolytes are continuously formed. Hence, the SEI reformation and the electrolyte decomposition are continuously restocked (1).

A considerable amount of research has been conducted to produce reliable solutions to the issues mentioned. One solution that has been the focus of much attention is the production of silicon (Si) in various nanostructures, such as nanowires, nanostructured silicon, and hollow and porous silicon structures. Being at the nanometer scale, these Si structures are incredibly useful, as they lessen mechanical stress with ease, and are known to be easier to lithiation and diffuse (6). Despite these benefits, nanosilicon

structures have a great downside to them: their high surface area causes massive capacity losses and excessive SEI formation (i), lower volumetric energy density (ii), and their complex and cost efficient synthesis methods that are difficult to scale (10). Alternatively, the focus has shifted to considering the availability, lower cost, and higher tap density of micron-sized silicon particles. These particles can be sourced from industrial processes, such as the cutting of silicon wafers, making them economically viable and environmentally friendly for widespread use. Higher tap density affords volumetric benefits, compared to nanosilicon, which is important for electric vehicle use. However, devices fabricated from micron-sized silicon are prone to mechanical failures due to increased cracking as the capacity fades faster (10). More innovative, and more importantly, more scalable approaches to improving cycling stability, as well as interfacial stability, also need to be developed.

From all the explored strategies, modifying silicon anodes with graphene has proven among the most successful. Among its numerous outstanding characteristics, graphene has excellent electronic conductivity (~10^6 S m^{-1}), high mechanical strength (~130 GPa), flexibility, and large specific surface area (up to 2630 m^2 g^{-1}). These properties are particularly useful in overcoming the limitations associated with silicon. Graphene can form a conductive network that sustains electron flow, even when silicon particles are fractured, act as a mechanical buffer to accommodate volume expansion, and stabilize the SEI by serving as a protective layer that restricts direct silicon-electrolyte contact which increases SEI growth (1). Graphene also has the capacity to create three dimensional structures (foams, aerogels, wrinkled multilayers) in which micron-sized silicon particles are embedded, thereby promoting the electrode's architectural fidelity and high areal capacities (10). The potential of graphene–silicon composites is experimentally substantiated by recent studies. Wrinkled multilayer graphene coatings on commercial silicon microparticles improved cycle life while maintaining high areal capacity. rGO-encaged micron-sized silicon composites showed improved rate capability and capacity retention. Coal-derived graphene foams with micron-sized silicon showed outstanding electrochemical performance and provided a low-cost, scalable solution. Graphene is shown to resolve silicon's intrinsic problems while maintaining compatibility with scalable electrode production, proving industrial relevance.

In conclusion, the remarkable potential of silicon as an anode material for next-generation lithium-ion batteries remains significantly underexploited. This is due to silicon's tendency to mechanically deteriorate, its inadequate conductivity, and the challenges associated with interfacial instability. Micron-sized silicon, although more accessible and cost-effective, still requires supplementary stabilisation methods to overcome its drawback. Graphene serves as a conductive matrix, mechanical buffer, and solid-electrolyte interphase (SEI) stabiliser, offering a valuable solution. This thesis aims to investigate the possibility of improved commercial micron-sized silicon particles combined with graphene for the development of high-performance, industrially scalable silicon anodes for advanced lithium-ion batteries.

2 Literature

2.1 Silicon Anodes in LIBs

The lithium ion battery (LIB) is preferred in portable electronics and electric vehicles (EVs) because of its high energy density and long cycle life. However, the energy density in the current lithium ion battery (LIB) is restricted because of the graphite anodes, which has a theoretical capacity of just 372 mAh g^{-1}. This is an obstacle to the development of higher capacity LIBs which are critical for long range EVs and for large-scale renewable energy storage (1). One of the anode materials that is Silicon (Si) has a theoretical capacity of about 3579 mAh g-1 (for $Li_{15}Si_4$), which is almost ten times higher than that of graphite, which makes it a stronger contender than graphite for the anode. Its volumetric capacity (about 2190 mAh cm^{-3}) is also very useful for constrained space applications (8). Silicon is also abundant, environmentally safe, and can be used in the fabrication of electrodes. These makes silicon a promising material when it comes to replacing or supplementing graphite in the commercial LIBs.

Certain remarkable characteristics of silicon also constitute its disadvantages also.
The previously discussed negatives comprise the following:

- An extreme large volumetric expansion of about 300% when the battery is fully lithiated, which results in a lot of mechanical stress, cracking, and pulverization of the particles.
- An extremely low conduction of electric current which greatly decreases the rate capability of the silicon batteries.
- Repeated mechanical fracture, along with exposure of new surfaces to electrolyte, leads to unstable SEI formation which consumes Lithium ions, hence lowering Coulombic efficiency. (3)These issues must be resolved for silicon to become a commercially viable anode material.

2.2 Micron Sized Silicon Vs Nano-silicon

Research into silicon anodes have mainly focused on nanostructured silicon materials, such as nanoparticles, nanowires, and porous silicon architectures, as nanosizing is widely regarded as a means to mitigate the significant volume expansion linked to lithiation, thereby improving mechanical stability during cycling (11). Despite these benefits, both nano- and micron-sized silicon anodes encounter significant difficulties that restrict their practical utilisation in lithium-ion batteries.

A significant challenge is the excessive development of the solid electrolyte interphase (SEI), especially in nanosilicon systems with elevated specific surface area, resulting in considerable irreversible lithium consumption and, therefore, diminished first-cycle Coulombic efficiency (1) , nanostructured silicon generally has a low tap density, which considerably diminishes the attainable volumetric energy density of the electrode, notwithstanding its elevated gravimetric capacity (12)(Moreover, the synthesis of nanosilicon frequently entails intricate fabrication methods and elevated production expenses, including vapour deposition, templating, or chemical etching processes, which significantly constrain scalability and commercial viability (8)

Micron-sized silicon particles (1-25 μm), on the other hand, are commercially available and inexpensive, having been derived from the remains of silicon wafers post-

processed. Their greater tap density gives them greater promise for volumetric capacity in practical electrodes (7). Their micron-sized particles are, however, more likely to fracture due to volume expansion and hence, pose the need to be combined with structural and conductive materials that mitigate these issues (10)

2.3 Synthesis and Processing Methods

Strategies including carbon-based graphene coatings have been extensively studied as effective methods to enhance the electrochemical performance of micron-sized silicon anodes, particularly by boosting electrical conductivity and reducing mechanical breakdown during cycling. The ball-milling-assisted graphene coating technology has been shown to be scalable and suitable with industrial applications for the production of graphene-coated silicon microparticles. This process involves the mechanical mixing of silicon particles with graphene oxide (GO), facilitating the physical anchoring of GO sheets onto the silicon surface, subsequently followed by thermal or chemical reduction to produce conductive reduced graphene oxide (rGO) layers. This approach is appealing because of its simplicity, scalability, and compatibility with commercial silicon powder (6)

A further efficient carbon-based method is the hydrothermal self-assembly technique, wherein graphene oxide is uniformly adsorbed onto silicon particles in an aqueous medium and subsequently reduced to reduced graphene oxide (rGO) under hydrothermal conditions. This technique facilitates the application of conformal graphene coatings and the development of interconnected conductive networks, hence improving charge transport and accommodating the significant volume expansion of silicon during lithition and delithiataion

Chemical vapour deposition (CVD) processes can produce high-quality graphene coatings; nevertheless, they are typically impractical for large-scale silicon anode production due to elevated processing costs, intricate working conditions, and restricted scalability.Thus, solution-based and mechanically assisted graphene coating techniques are the most feasible and commonly utilised approaches for the fabrication of silicon–graphene composite anodes for lithium-ion batteries (8)

2.4 Performance Evaluation of Electrochemical of Graphene–Si Composites

The electrochemical performance of reduced graphene oxide (rGO)–silicon composites has been extensively studied, indicating their effectiveness in improving conductivity and cycling stability of silicon anodes. Si/rGO composites have initial discharge capacities of around 2200 mAh g^{-1} at a current density of 100 mA g^{-1}, maintaining approximately 852 mAh g^{-1} after 200 cycles at 500 mA g^{-1}, with a first-cycle Coulombic-efficiency of roughly 63% (13) Coal-derived graphene foam integrated with micron-sized silicon exhibits increased cycling stability and capacity retention relative to pure silicon after exceeding 100 cycles, contributing to the conductive and mechanically resilient graphene structure (10). Moreover, wrinkled graphene-coated silicon microparticles possess flexible carbon coatings that allow volumetric expansion, leading to improved cycling stability and areal capacity performance (6)

2.5 Electrode Fabrication and Mechanical Aspects

Aside from the design of the materials, electrode fabrication has a major effect on performance. Electrode cohesion and porosity are influenced by the slurry consistency, strainers, binders, and calendaring.Unlike PVDF, the elastic binders CMC/SBR and PAA sheath holders that display superior adjustable elasticity and adhesion (14), and the ideal range of solids for slurries is between 40-60 wt% this range ensures coatability and uniformity. In graphene composites, conductive additives can be lower, but minor amounts of carbon black are beneficial to the slurry rheology and electrode calendaring needs to strike the right porosity to density ratio to accommodate the volume expansion of Si.

2.6 Electrochemical Tests for Graphene – Silicon anodes

Electrochemical testing quantifies the performance, kinetics, and stability of electrode materials for lithium-ion batteries (LIBs). The use of such anodes is necessitated by their high theoretical capacity (~ 3579 mAh g^{-1}, for $Li_{15}Si_4$) and interim mechanical and interfacial issues associated with large volume expansion (from ~c.a., 300%) during lithium insertion/desertion. The presence of graphene as a conductive and flexible coating drastically changes the electrochemical performance of the composite, resulting in enhanced capacity retention, impedance and charge-transfer kinetic, and long-term cycling stability (15). The principal electrochemical methods to study these composites are Cyclic Voltammetry (CV), Electrochemical Impedance Spectroscopy (EIS) and Cycle Life Testing as well as Capacity Retention (CR). Each of these gives a complementary view on the electrochemical and physical behavior of the cell.

2.6.1 Cyclic Voltammetry (CV)

Cyclic Voltammetry is a widely-used diagnostic technique that provides information about the redox behaviour and lithiation/delithiation kinetics of an electrode. In CV a potential is linearly varied with time between two limits and the current drawn therewith can be read. The dependence of the I (current response) on the E (applied potential), is an indication of any reversible electrochemical reaction, charge transfer kinetics and phase transitions that may occur within the electrode material during this process (16).

The CV response is significantly changed with graphene coating as the first-cycle reduction peak (pertaining to SEI formation) is at a higher current, indicating that the deposition of the SEI layer has been retarded by graphene as a protective barrier and the following cycles present well overlapped redox peaks, demonstrating reversibly with little electrode degradation in the long-term use (15) while , the integrated area in CV curve is almost unchanged during repeated circulation, which further illustrates its high coulombic efficiency and stable charge storage. A symmetric current–potential loop represents the equilibrium between anodic and cathodic reactions, suggesting that the electrode could have a stable and reversible Li-insertion reaction. This symmetry and repeatability across repeated operation cycles demonstrate that the graphene coating indeed provides an efficient strategy to alleviate volumetric strain and preserve electronic conduction, which is in line with previous reports for rGO–Si composites (17).

2.6.2 Electrochemical Impedance Spectroscopy (EIS)

Electrochemical Impedance Spectroscopy is an effective method applied to assess internal resistances within the battery such as ionic resistance (R_s), SEI solid resistance (R_SEI) and charge-transfer resistance (R_ct) (16). EIS involves applying a small amplitude AC potential across different frequencies (usually from 1 MHz to 10 mHz), and monitoring the impedance response.

The Nyquist plot ($-Z''$ vs. Z') will usually shows a real-axis high-frequency intercept, solution resistance (R_s), and a semicircular arc in the middle frequency region, attributed to R_ct and SEI layer resistance and a low frequency region is a tail, which indicates lithium-ion conduction (Warburg impedance).

For a well-performing Si-rGO electrode, the diameter of the semicircle (inversely proportional to R_ct) is small and constant during cycling, suggesting fast charge-transfer behaviour and a narrow half circle in the initial cycle suggests good interfacial contact and conductive network between active materials due to that of Gs.The linear tail at low frequency is attributed to the uniform of lithium during within the electrode, which demonstrates the homogeneous coverage of graphene and inhibits crack (9). A small semicircle at near the origin and an almost constant impedance with the cycling in your EIS results, confirms low degradation by assuring stability of Si–graphene interface its high conductivity. This behavior indicates that the electrode still keeps a good electrical contact and ionic transport after multiple cycle numbers, which is crucial for long cycles and battery reliability.

2.6.3 Cycle-life and capacity-retention

Cycle life testing consists of subjecting the battery to a series of repetitive charge and discharge cycles under controlled conditions while tracking changes in capacity and coulombic efficiency as a function of time. Which enable direct observation on structural robustness, electrode completeness, and interface uniformity in long-term operation.The capacity loss at the initial cycles for the silicon-based electrodes is attributed to mechanical strain and SEI formation. Nonetheless, graphene coatings largely inhibit the degradation kinetics by balancing volume change, sustaining conductance network, and stabilizing SEI (4) Studies show that, from your observations, the slight and controlled reduction in capacity indicates stable interfacial bonding and mechanical integrity of the composite. The stable coulombic efficiency (>99% after formation) also verifies reversible lithiation/delithiation without significant loss of lithium.

The high rate performance and capacity retention at high current densities are indicative of excellent electronic and ionic conductivity in the graphene network, which is essential to fast applications like electric vehicles. A short retention curve with negligible flattening over long cycles may be an indication of good structural robustness and electrochemical stability.These electrochemical tests are combined to gain a full picture of the electrode performance. From the CV, all redox reactions are reversible and stable, and resistive losses are quantified by the EIS, and stable charge-transfer properties are confirmed, and also, cycle life-testing is used to evaluate long-term mechanical and interfacial stability. Cycle performance reflects rate capability and resistance to the current of the composite.

The electrochemical findings—namely, the stable cyclic voltammetry (CV) peak profiles, the consistently small semicircles noted in the electrochemical impedance spectroscopy (EIS) measurements, and the capacity retention observed over multiple cycles—indicate that the graphene coating enhances the electrochemical stability of the silicon anode during cycling. Although these results do not eradicate all degradation processes, they suggest a diminished severity of prevalent failure mechanisms commonly linked to silicon anodes, including particle breakage, ongoing SEI growth, and gradual loss of electrical contact.

The observed patterns align with findings documented in the literature. indicated that rGO-coated micron-sized silicon anodes maintained approximately 852 mAh g^{-1} after 200 cycles, while the uncoated silicon electrodes demonstrated capacities below 300 mAh g^{-1}. This enhancement was described to the existence of a continuous graphene network that facilitates the preservation of electrical connectivity and structural integrity during successive lithiation and delithiation cycles. These data suggest that graphene coverings have advantages beyond merely improved electrical conductivity. The graphene layer may function as a mechanically flexible buffer and a protective interfacial layer, facilitating the accommodation of silicon volume fluctuations and mitigating interfacial deterioration. Graphene-coated micron-sized silicon anodes exhibit enhanced cycle stability relative to uncoated silicon; nonetheless, additional long-term investigations are necessary to comprehensively evaluate durability under prolonged cycling circumstances.

Table 1 - Different electrochemical tests behaviour

Test	Measured Parameter	Graphene–Si Impact	Interpretation
Cyclic Voltammetry (CV)	Reversible lithiation/delithiation potential peaks	Stable, overlapping redox peaks	High reversibility and minimal degradation
Electrochemical Impedance (EIS)	Charge-transfer resistance (R_ct)	Small semicircle, steady over cycles	Good electronic/ionic conductivity
Cycle Life Test	Capacity vs. cycle number	Slow capacity fade	Mechanical and interfacial stability
Capacity Retention (CR)	Capacity under varied current densities	High capacity at higher current	Robust rate performance

3 Methodology

3.1 Overview

In this chapter, we describe the full process of synthesis, treatment and evaluation of graphene-coated Si particles as a potential high performance anode for LIBs. The procedure combines surface modification, graphene attachment, chemical reduction and electrode preparation to enhance the electrical conductivity and mechanical stability of micron/nano silicon particles.

The process is decomposed into the stages:

1. Silanization with APTES enhancing the reactiveness of surface and adhesion between graphene to it.
2. Uprooting and cleaning of graphene oxide (GO) to get the uniform suspension for homogenous coating.
3. Reduction of GO prepared by use of hydrazine hydrate to reduce GO and convert it into rGO which is electrically conducting.
4. The coated films were then dried and annealed after treatment, and subsequently electrodes were made for electrochemical measurements.

The entire schematic diagram of the synthesis process is shown in Figure-1

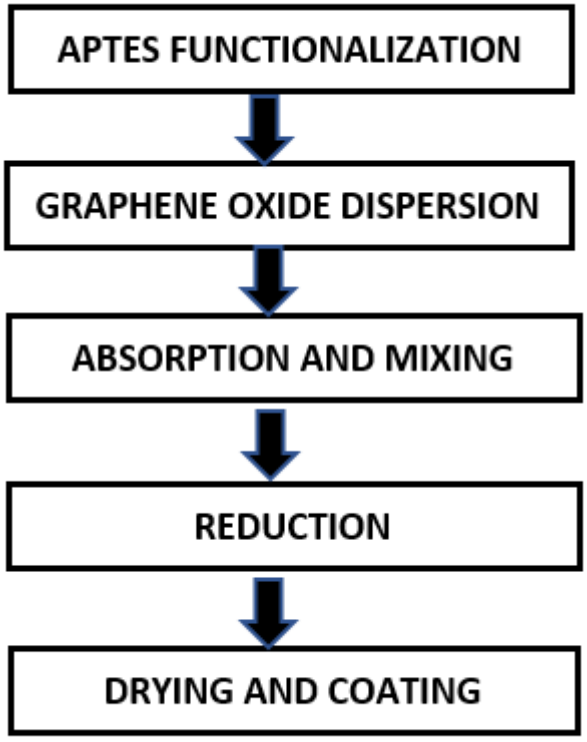

Figure 1 - Schematic diagram of synthesis process

Table 2 - Different stages of synthesis process and their outcome

Stage	Step	Main Reaction / Mechanism	Outcome
Silanization	APTES	Covalent bonding via Si–O–Si	Amine-functional Si
Coating	GO adsorption	Electrostatic & hydrogen bonding	Si@GO composite
Reduction	Hydrazine hydrate	Chemical GO → rGO	Conductive Si@rGO
Electrode	Slurry casting	Uniform film on Cu foil	Working electrode

3.2 Treatment of Silicon Particles

3.2.1 Silanization with APTES

Through surface silanization, the amino functionalities ($–NH_2$) are introduced to form better connection of Si with GO by hydrogen bonding and electrostatic attraction.

Procedure:

- Distribute 2 g of washed Si powder in 50 mL of a 5 wt% APTES solution in toluene.
- Reflux the suspension for 2 h at 110 °C with continuous magnetic stirring.
- The mix was cooled to room and centrifuged.
- Sequently wash the above samples with toluene, methanol and DI water to remove unreacted APTES.

Chemical mechanism:

$$Si–OH + (EtO)_3–Si–(CH_2)_3–NH_2 \rightarrow Si–O–Si–(CH_2)_3–NH_2 + 3\ EtOH$$

This reaction results in covalent Si–O–Si formation, rendering a stable amine terminated surface.

3.2.2 Coating with GO

Graphene oxide is hydrophilic but has a tendency to aggregate due to the oxygenated species (epoxy/hydroxyl/carboxyl) it bears. Appropriate dispersion guarantees the homogeneous Si coating.

Procedure:

- The washed Si after APTES coating is then stirred in magnetic stirrer and GO is added step by step until desired wt% is achieved in that particular step or until Si takes graphene as its coating uniformly and GO is ultrasonicated before adding to the Si for better coating.
- The mixture was centrifuged (4000 rpm, 10 min) to eliminate large aggregates. The supernatant with homogenously spread GO was used for coating purposes.

Mechanistic note:

Stability of the GO suspension is due to electrostatic repulsion of negatively charged carboxylate groups. Maintaining the pH level close to neutral during this stage avoids aggregate formation in early phase.

3.3 Synthesis of Si–Graphene Oxide Composite

3.3.1 Adsorption and Mixing

Procedure:

- Firstly, APTES-treated Si (1 g) was added to the GO dispersion (~50 mL) with vigorous stirring.
- Protonation of amine groups ($–NH_3^+$) leads to an increased electrostatic interaction with negatively charged GO sheets, resulting in the formation of a uniform coating.

$$NH_2–Si + H^+ \rightarrow NH_3^+–Si \text{ (positively charged)}$$

- Mix the above solution at room temperature for 8 h, by which complete GO should have adsorbed onto Si surfaces.

3.3.2 Washing and Drying

After coating:

- Filter, and wash successively with DI water and methanol until the washings become neutral and colourless.
- Vacuum-dry the GO-coated Si (Si@GO) at 80 °C overnight.

Observation: The color of the powder turns from gray (nude Si) to brownish-gray, indicative that GO uniformly covers it.

3.4 Reduction of Graphene Oxide (GO → rGO).

The electric conductivity of GO is insufficient on account of the oxygenated nature in its structure. The reduction returns the π-conjugated carbon network.

Chemical reduction process:

$$GO + N_2H_4 \rightarrow rGO + N_2 + H_2O$$

Procedure:

- Disperse Si-GO (~1 g) in 30 mL DI water.
- Dropwise add 1 mL hydrazine hydrate at stirring.
- The suspension is then heated to 95 °C and allowed to reflux for 2–3 h.
- When finished, allow to cool at room temperature.
- Filter and wash well with DI water and methanol to remove free hydrazine.
- Dry in vaccum at 80 °C for 12 h.

Results and Discussion: The colour changes from brown (GO) to blackish dark indicating the reduced GO (rGO).

Safety: Hydrazine is highly toxic and flammable, and reactions were conducted in a fume hood employing appropriate safety precautions.

3.5 Electrode Fabrication

The electrodes were prepared by a water based slurry method that allows for scaling up because it provides advantages for scalability, safety, and environmental sustainability. Aqueous processing, in contrast to traditional solvent-based systems like N-methyl-2-pyrrolidone (NMP), eliminates the necessity for hazardous organic solvents, thereby minimising environmental consequences and improving handling and processing. Moreover, water-based slurries facilitate reduced production costs and exhibit greater compatibility with industrial-scale electrode fabrication. The application of a water-based slurry technique facilitates the advancement of a scalable and practically applicable silicon-graphene anode manufacturing process.

Composition:

- 80 wt% Si-rGO composite
- 10 wt% Super P (conductive carbon)
- 10% by weight of a binder (CMC/SBR in 1/1 ratio).

Procedure:

- Distribute Super P and binder in considered ratios in mortor along with Si-rGO composite and mix it well.
- Make the mixture uniform by mixing it well and adjusting its consistency by adding DI water if required.
- Spread the slurry on a copper foil using a doctor blade (wet thickness ≈100 μm).
- Dry at 80 °C for 12 h in vaccum oven, and then calendar at moderate pressure to obtain the density uniformity.
- Punch electrodes (12 mm diameter) and weight for mass loading measurements (typically 1–2 mg cm^{-2} for lab-level screening).

3.6 Coin Cell Assembly

The 2032-type half-cells were fabricated in an argon-filled glovebox (O_2, H_2O < 0.1 ppm) with, (19) (20) (21) (22)

- Working electrode: Si-rGO on Cu foil
- Counter/reference: Lithium metal foil
- Separator: Glass Fiber
- Electrolyte: 1 M $LiPF_6$ in EC:DMC (1:1 v/v) with 10 wt% FEC

Cells were rested for 12 h prior to electrochemical evaluation.

3.7 Electrochemical Measurement Protocol

Galvanostatic charge–discharge (GCD)

- Voltage region: 0.01–1.5 V (vs Li/Li^+)
- cycles at 0.05C were applied for the formation of the samples.
- Cycle life test: 0.5C/200 cycles

Cyclic Voltammetry (CV)

- Scan rate: 0.1–1 mV s^{-1}
- Voltage range: 0.01–3.2 V
- Purpose: Analyze lithiation/delithiation peaks

Electrochemical Impedance Spectroscopy (EIS)

- Frequency: 100 kHz – 10 mHz
- Amplitude: 10 mV
- Before cycling, after assembly and after 100 cycles

3.8 Summary

The established method offers a robust strategy for fabricating advanced graphene–silicon composites for lithium-ion battery anodes. Key innovations include:

- Surface treatment by APTES for improved adhesion of graphene.
- GO adsorption to promote coating uniformity.
- Chemical reduction using hydrazine as a reductant to recover the electrical conductivity.

This method provides the strong interfacial adhesion, homogeneous coating and excellent reproducibility, which are indispensable for stable electrochemical cycling.

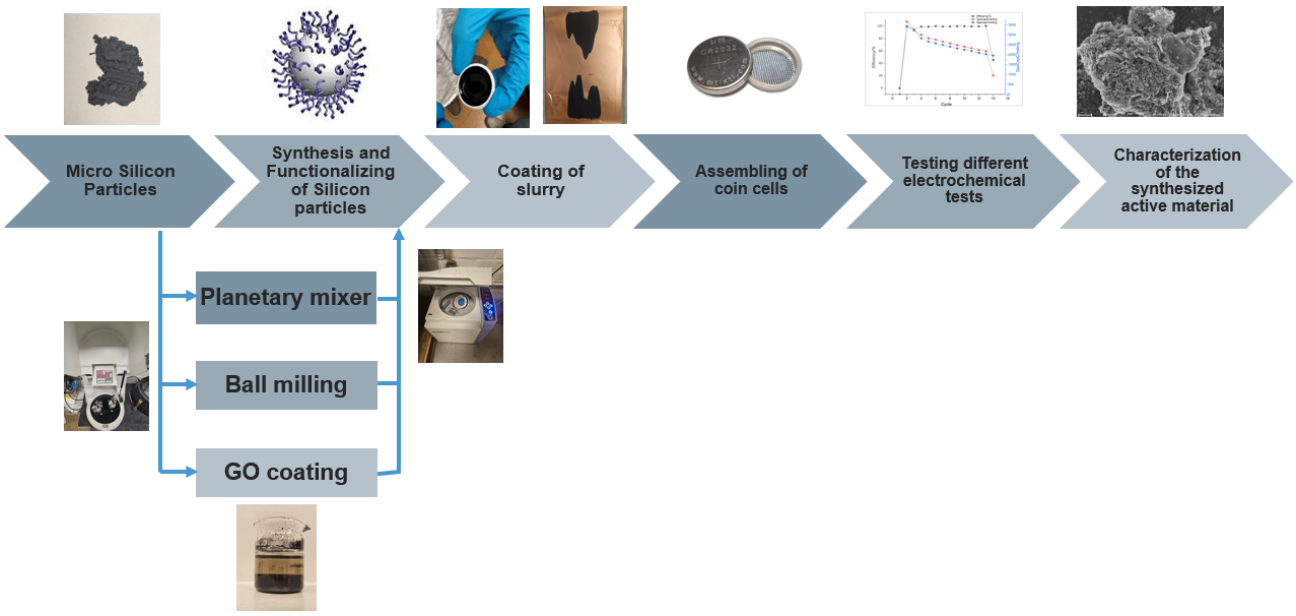

Figure 2 - Pictorial illustration of the step-by-step synthesis proceduree

Table 3 - Different materials used in the synthesis and their purpose

Material	Specification / Source	Purpose
Silicon powder (micron size)	1–5 µm, ≥99%, commercial	Active material (bulk comparison)
Graphene oxide (GO)	Synthesized via modified Hummers' method / commercial	Graphene precursor
APTES ((3-Aminopropyl)triethoxysilane)	99%, Sigma-Aldrich	Surface silanization
Toluene	Analytical grade	Solvent for silanization
Methanol	Analytical grade	Washing and cleaning
Hydrazine hydrate ($N_2H_4 \cdot H_2O$)	80%	Chemical reduction of GO
Deionized water (DI)	Resistivity >18 MΩ cm	Washing and dispersion medium

4 Results

4.1 Overview

This chapter contains the experimental results from assembling and characterizing graphene-coated silicon (Si) anode materials, followed by their electrochemical testing. The results will focus primarily on particle processing method (ball-milled vs. commercial), presence of a graphene coating, and the type of coating method (planetary vs. conventional mixing) in determining the electrochemical performance and microstructural sustainability of Si-based anodes.

The performance will be assessed based on standard electrochemical tests: cyclic voltammetry (CV), electrochemical impedance spectroscopy (EIS), and galvanostatic charge-discharge (GCD) cycling. All electrodes are made using the same binder and same slurry conditions to ensure differences in results are related to coating method and material processing effects.

- Ball-milled Si particles are typically found to be smaller in particle size compared to commercial micron-sized Si, thus allowing for better dispersion of graphene coating and better adhesion of the coating to the particle.
- Graphene-coated Si electrodes consistently outperform uncoated Si in terms of reversible capacity and stability due to increased conductivity and suppression of SEI delamination.
- Planetary mixed coating leads to a less consistent distribution of graphene than when using acid-assisted conventional mixing method of coating that allowed for complete conformal coverage of Si by the graphene sheets.
- Observed agglomeration of graphene oxide (GO) along with partially coated surfaces suggest that the process needs to be tuned to achieve consistent coatings that are uniform and hold for extended duration.

4.2 Comparison of Ball-Milled and Commercial Silicon After Graphene Coating

The first exploratory experimental comparison was of ball-milled Si compared to commercial micron-sized Si with a graphene coating. Morphological and surface features. According to SEM the Si particles from the ball milling were irregular sizes but were homogenized at a smaller size (~1−3 μm) from mechanical size reduction, yielding higher surface area and better adhesion of the graphene. In contrast, the commercial Si particles (as received) (~5−25 μm) were smooth facing and angular, yielding less uniform dispersion of graphene. The graphene layer appeared wrinkled and partially interconnected allowing for conductive bridges between Si particles. The smaller overall size of the ball-milled Si particles allowed for a healthier contact between the graphene and Si allowing for less ionic isolation between cells while improving electron transport. Conversely, the small particle size may create greater surface reactivity, rendering thicker SEI layers being formed during early cycles if the coating surface is not continuous.

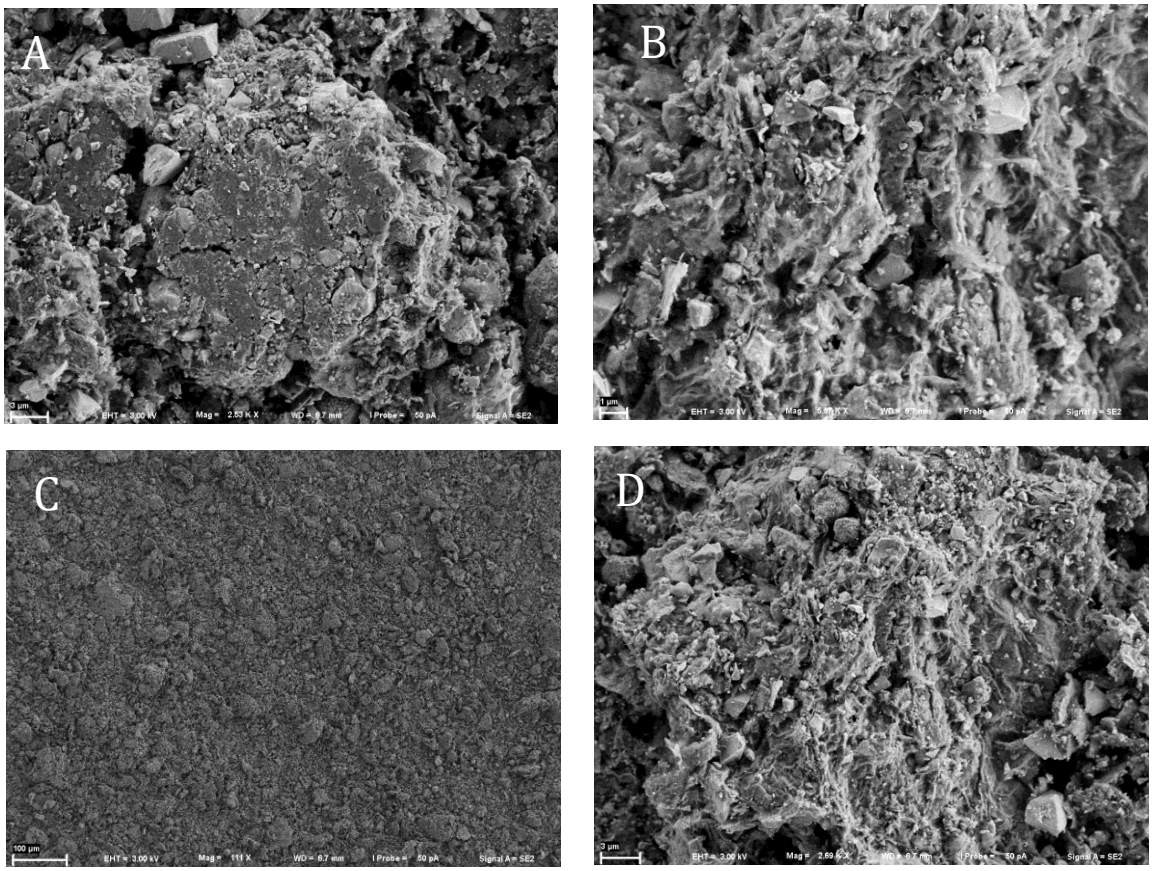

Figure 3 - SEM images of commercial silicon particles coated with graphene-oxide after ball milling

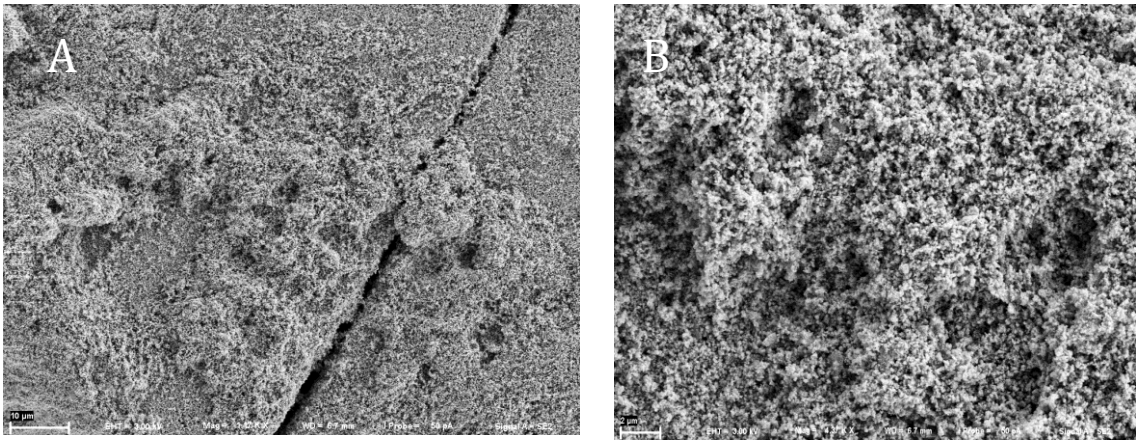

Figure 4 - SEM images of commercial silicon particles coated with graphene-oxide during ball milling

Electrochemical performance

In CV test results, both samples exhibited lithiation and delithiation peaks near 0.1 V and 0.45 V vs. Li/Li^+, respectively; However, the peak intensity for the ball-milled and graphene-coated Si electrode were sharper and more stable in respective cycles suggesting improved charge transport kinetics and possibly a more stable SEI.

In cycling tests, the ball-milled and graphene-coated Si maintained ~70% of the starting capacity after 200 cycles and the commercial Si retained about 55-60%. The evidence

provided above clearly indicates that the size of the particles and the uniformity of the coating are both key contributors to preventing the degradation that is typically a result of Si expansion during lithiation.

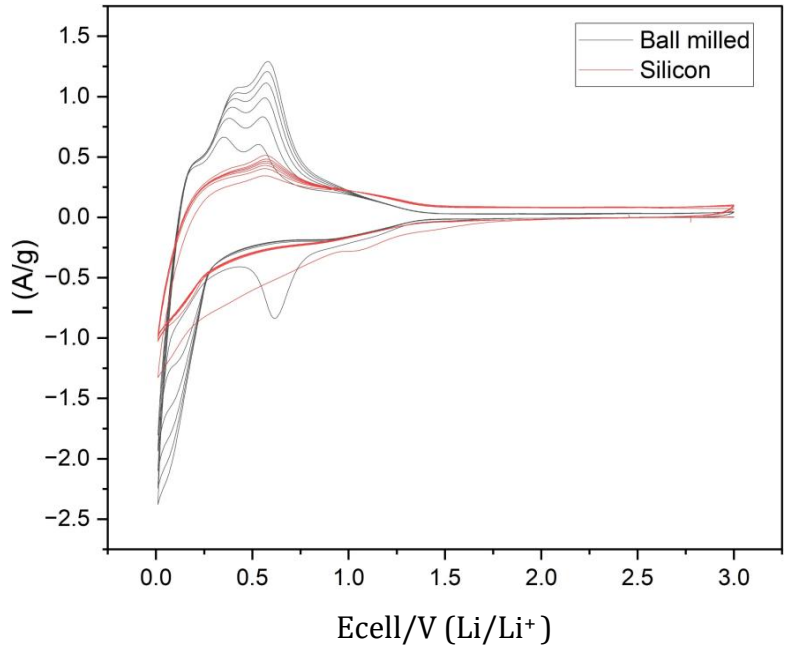

Figure 5 - Cyclic Voltammetry comparison of ball milled silicon together with GOand separately coated after ball-milling

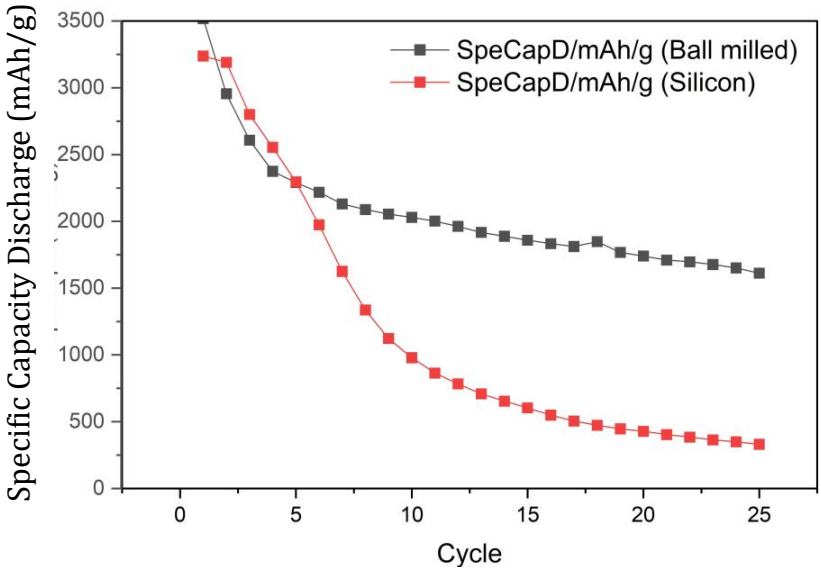

Figure 6 - Cycling performance comparison of ball milled silicon together with GO and separately coated after ball-milling.

4.3 Comparison of Ball Milled Silicon (BMS) Uncoated vs. Graphene Coated

The second study was conducted comparing BMS Si without any coating to BMS Si coated in hydrazine hydrate reduced graphene oxide (rGO).

4.3.1 Morphology and Interfacial Structure

The surface of the uncoated BMS appeared to have relatively rough particle surfaces and visible microfractures were observable in the particles after the first cycles. In contrast, the rGO BMS appeared to have a smooth surface with most particles intact with a continuous wrinkled carbon matrix that attached neighboring particles in a calico like pattern.

The matrix acts as a mechanical buffer and allows electronic connectivity through the matrix during the ~300% volume expansion and contraction of the Si during cycling.

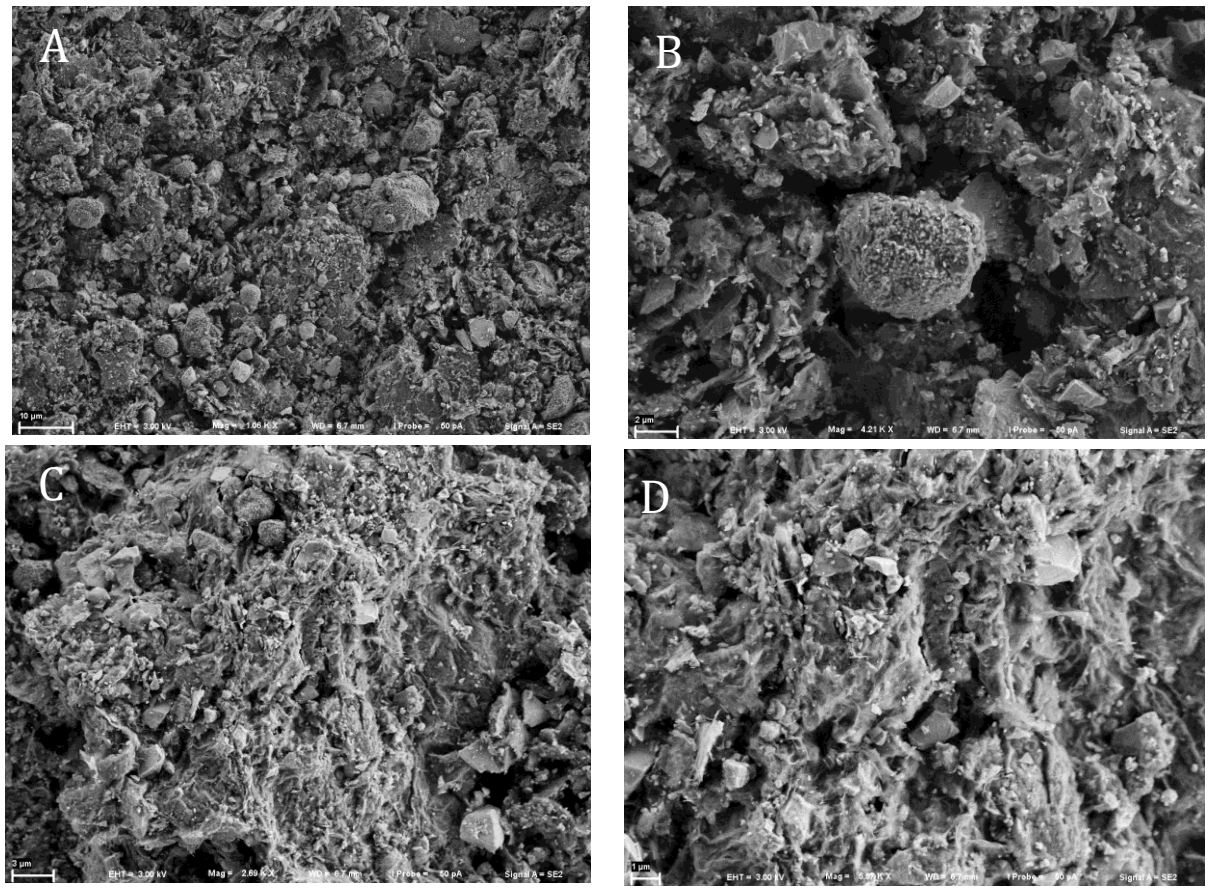

Figure 7 - SEM images of commercial Silicon GO coated after Ball-milling

4.3.2 Electrochemical performance

The cyclic voltammetry profiles of ball-milled silicon and commercial silicon electrodes obtained over several cycles within the voltage range of 0.01–3.0 V. Both electrodes demonstrate a cathodic current at low potentials (<0.2 V), indicative of lithium insertion into silicon and the first creation of the solid electrolyte interphase (SEI). Anodic peaks detected between about 0.3 and 0.6 V correspond to the delithiation of LixSi phases. The ball-milled silicon electrode exhibits an enhanced current response and improved overlap of consecutive CV cycles relative to commercial silicon, signifying more stable electrochemical performance during cycling. In contrast,

the commercial silicon electrode exhibits reduced current intensity and a less uniform peak progression throughout cycles.

The uncoated BMS Si showed a high capacity initially(~2100 mAh g-1), however the capacity was very quickly lost after the 25 cycles, because the pulverised particles underwent an unstable SEI formation instead of having retained capacity, which is demonstrated by an initial cycle coulumbic efficiency (ICE) of ~55%, suggesting extensive electrolyte degradation. The BMS Si was coated in rGO and had a comparable initial capacity to the uncoated (~2200 mAh g-1). Additionally, the ICE increased significantly to ~70%, indicating less irreversible utilization of Li in the SEI formation compared to the uncoated. These findings substantiate that the utilized graphene coating confidently improves the durability of the electrode in addressing Si performance in an electrochemical system due to isolation from the liquid electrolyte and connections between Si particles and electrodes.

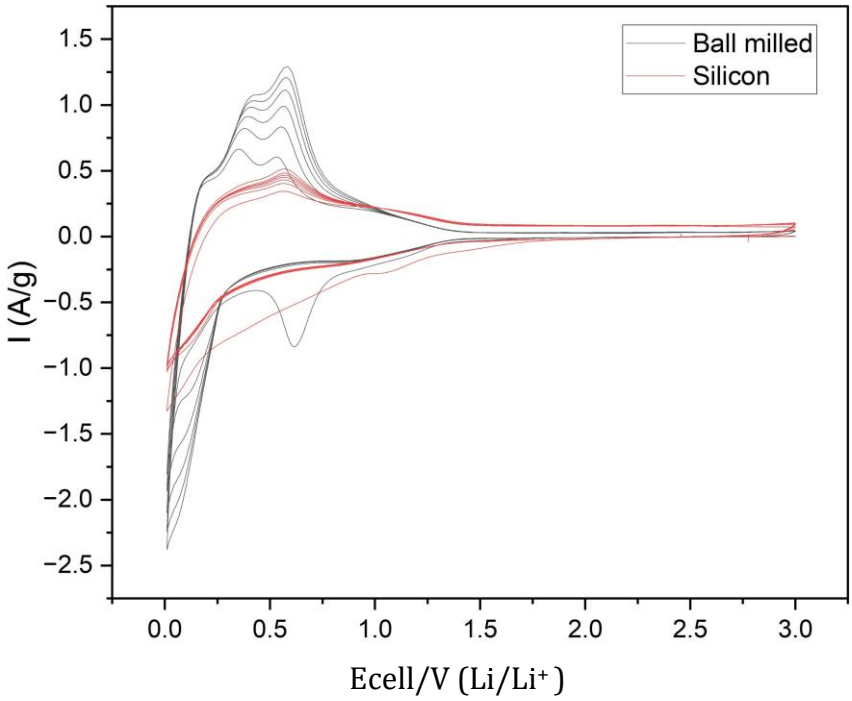

Figure 8 - Cyclic Voltammetry comparison of ball milled silicon without GO and silicon separately coated after ball-milling

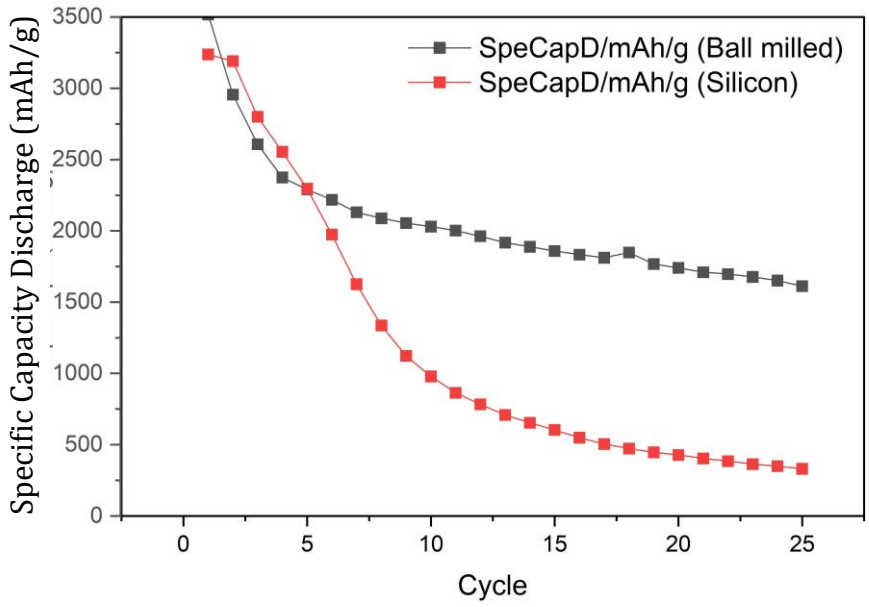

Figure 9 - Cycling performance comparison of ball milled silicon without GO and silicon separately coated after ball-milling

4.4 Comparison of Coating Method: Planetary Mixing vs Conventional stirring

The third phase of experiments assessed how directionally different methods of coating did in regard to dispersion and working electrochemical behaviour.

4.4.1 Coating uniformity and dispersion

When GO was introduced and utilized as a mix to coat Si using a planetary mixer, it was evident that there was some mixing at the end of the process, where it did begin to behave with uneven distribution and even agglomerating. Because of the centrifugal forces, when agglomeration occurred, despite GO attempting to lay down evenly on the surface of the Si, it would not lay down due to the combination of dryness and the forces applied. This leads to exposing Si, which was not subject to an SEI when cycling. Conversely, through the acid-assisted conventional mixing, there was a substantial shift in the coating, as it was more homogenous in appearance and exhibited stronger peaks of coverage and conformation.

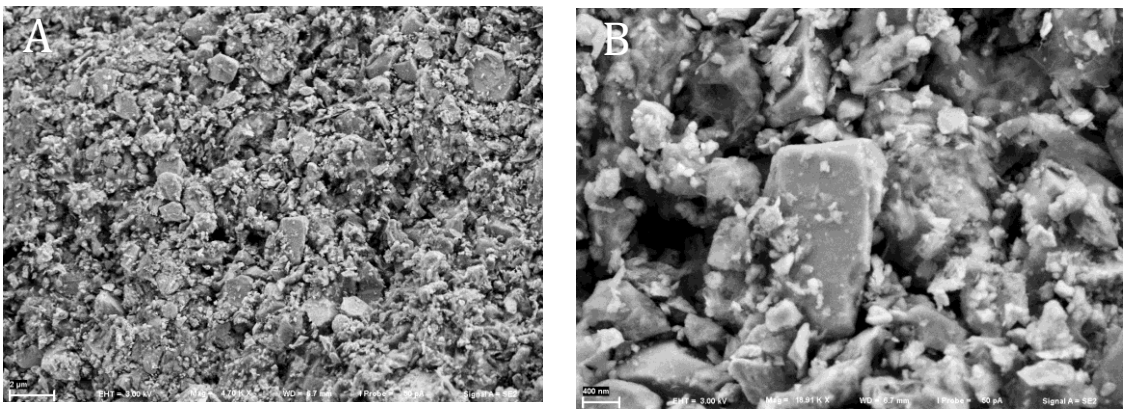

Figure 10 - SEM images of commercial Silicon GO coated with Planetray mixer coating method

4.4.2 Electrochemical behaviour

Cells made with the planetary mixing procedure found limited cycle stability and impedance, shown in the CV profile above, where the process yielded R_ct above to sub 200Ω after 50 cycles. As expected, the capacity showed considerable drop below 50% after 100 cycles, thereby acknowledging mechanical failure and interfacial performance failure reflecting uneven distributions of coating.

The results from the electrodes made through the acid-assisted method showed stable CV peaks, positions that remained constant, and intensities remaining constant when tested over 100+ cycles. Capacity retentions graced ~70% in high cycle counts, through ~200 cycles. When considering the chemistry of surface of the coating itself, it was clear that functionalization was crucial considering electrochemical behavior. Subsequently, when the graphene coated uniformly, even when there was diminished activity in the cycling process, it had uniform stability.

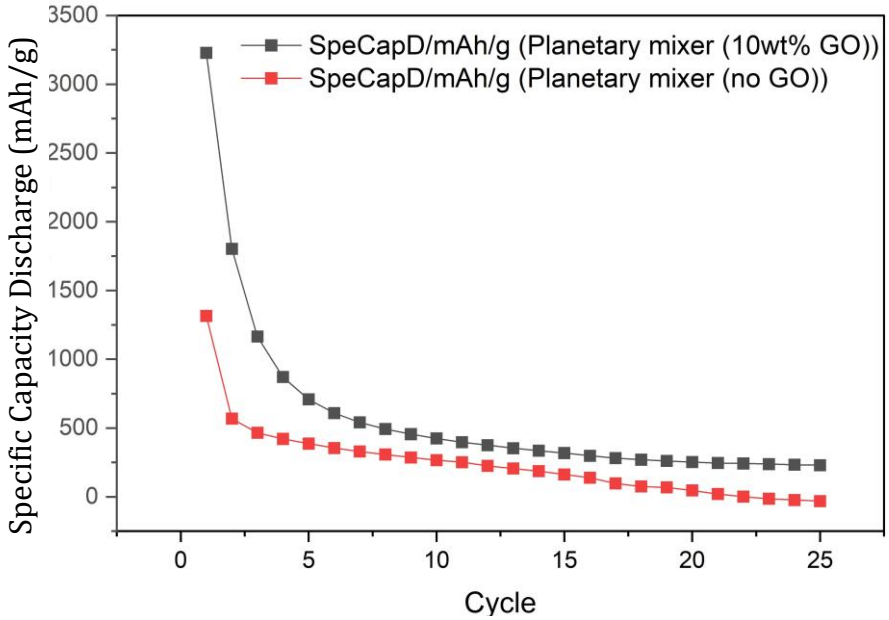

Figure 11 - Cycling performancey comparison of Silicon with 10wt% GO and no GO coated in planetary mixer method

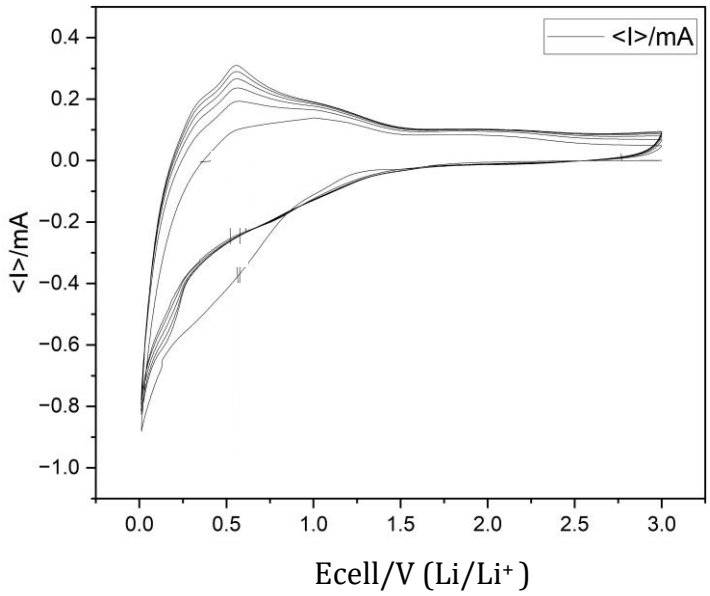

Figure 12 - Cyclic Voltammetry comparison of Silicon with 10wt% GO and no GO coated in planetary mixer method

4.5 Comparison of Various Levels of Graphene Coating Ratios (10wt% v/s 20wt% GO)

The SEM imaging was performed for the purpose of determining the morphological differences that result from the variation of GO content during the coating of silicon particles. Shown are the images of the surface morphology of silicon particles coated with 10 wt% GO on the left and with 20 wt% GO on the right.

From the data obtained from the coating of Si with 10wt%GO, it is seen that there is a thin but continuous wrinkled network of graphene covering the surfaces of the silicon's, the sheets of graphene appear to conform to the silicon and to be fairly uniformly dispersed throughout the coatings; the interconnected conductive structure created allows one to still see the morphology of the silicon itself. The structure of this coating is in line with moderate loading of GO having been coated on the silicon, with good dispersion and little agglomeration.

On the other side, the silicon particles coated with 20 wt% GO shows a substantial increase in thickness of the coatings and a much more clustered design. The sheets of GO exhibit much more folding, stacking and aggregating than for 10 wt% coated Si therefore providing much denser, yet less uniform coverage in this example. While many areas seem rather bulky, this is indicative of local re-stacking of GO as a result of the high loading of GO. While overall coverage is much greater due to the high loading of GO, the combination of GO layers results in a less uniform coating than was exhibited by the 10 wt% coated Si particles.

The morphological studies indicated that GO loading plays a critical role in the establishment of uniformity of coatings, dispersion of the sheets and connectivity of the particles.

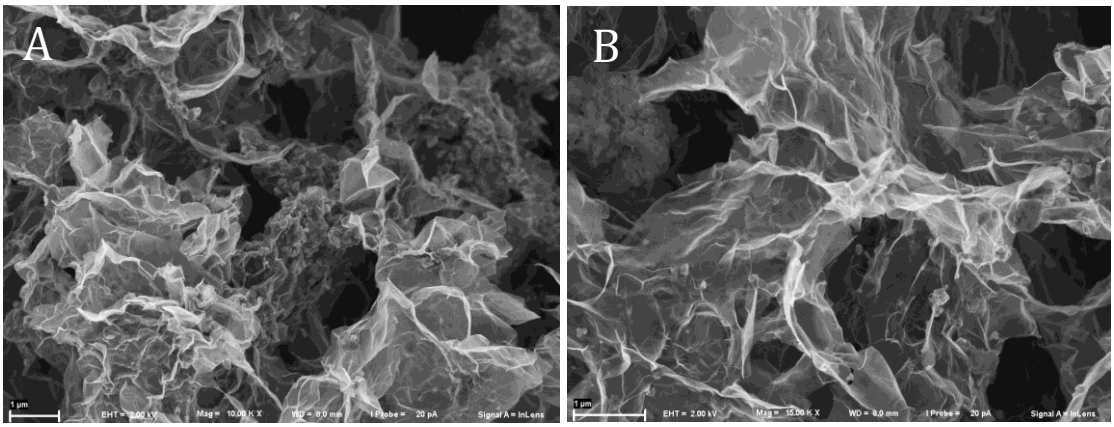

Figure 13 - Silicon coated with 10wt% GO

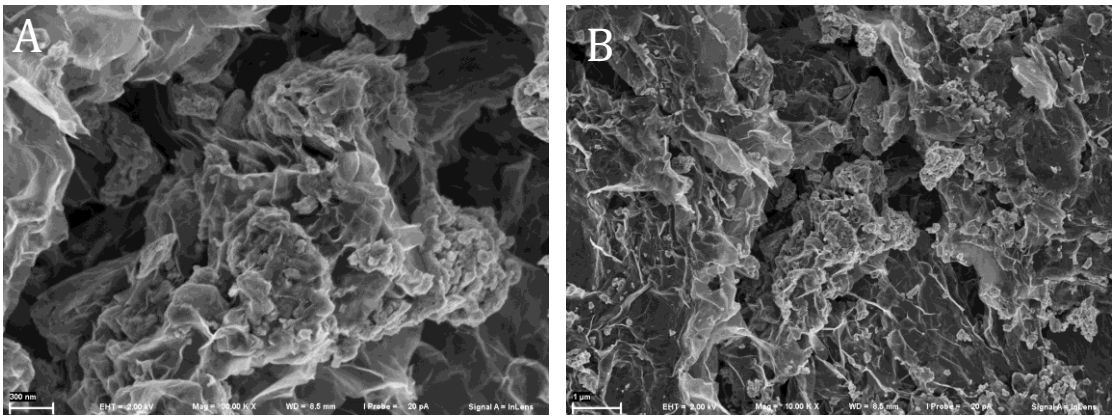

Figure 14 - Silicon coated with 20wt% GO

4.5.1 Electrochemical performance

The Si - 10wt%GO has an initial discharge capacity of approximately 3000mAhg^-1 and the Si - 20wt%GO has a slightly larger discharge capacity of approximately 2500mAhg^{-1}, both of which are higher than the reported discharge capacity for pristine silicon. However, there was a substantial difference in the amount of degradation of capacity between the two types of coatings. The 20wt%GO coating had a greater loss of capacity than the 10wt%GO after the first 10 cycles, from approximately 3000 to approximately 1400mAhg^{-1}, while the 10wt%GO coating had a much smaller loss of capacity (from approximately 2500 to approximately 1700mAhg^{-1}). At cycle 25, the 10wt%GO had a residual discharge capacity of approximately 1600mAhg^{-1}, greater than twice that of the 20wt%GO sample (approximately 900mAhg^{-1}). This data indicates that although the greater amount of GO used to create the Si-(GO) (10wt%) provided a greater initial discharge capacity due to the increased surface area available for Li+ adsorption, excessive amounts of GO also creates transport and structural constraints leading to a faster than normal rate of capacity fading.

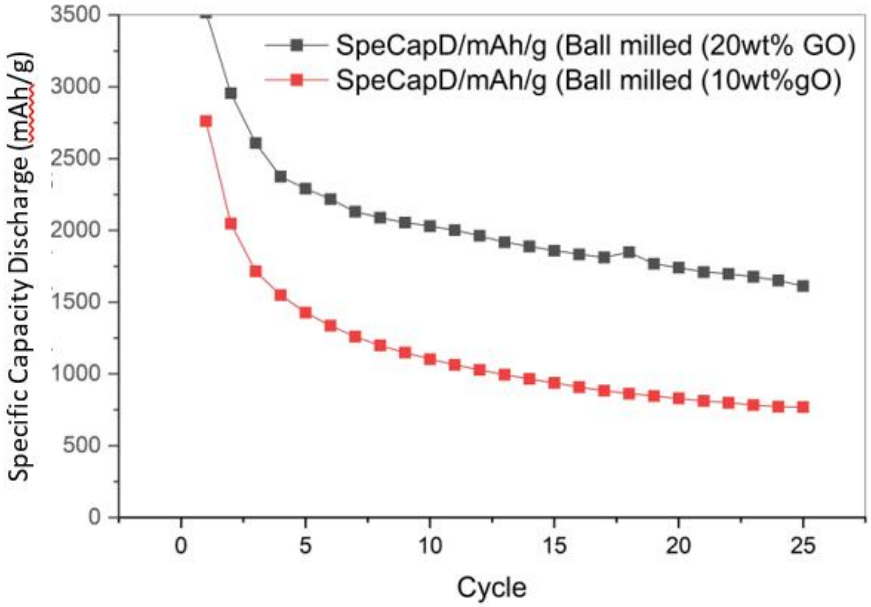

Figure 15 - Cycling performancey comparison of Silicon with 10wt% GO and 20 wt% GO

4.5.2 Electrochemical Impedance Spectroscopy (EIS)

The 10wt%GO coating had a smaller diameter semicircle compared to the 20wt%GO coating. In addition, the 10wt%GO had lower overall impedance and a well-defined linear region in the Warburg area at low frequency.The 20wt% GO sample displays. Large semicircle observed, indicating R.ct is higher and steep slope longer than 10 wt% GO, indicating that Li is diffused into the electrode at a slower rate. Because of this high impedance seen in the 20wt% GO, too much Graphene creates thickness in the conductive layer, preventing Ion Transport / creating interfaces with high Resistance

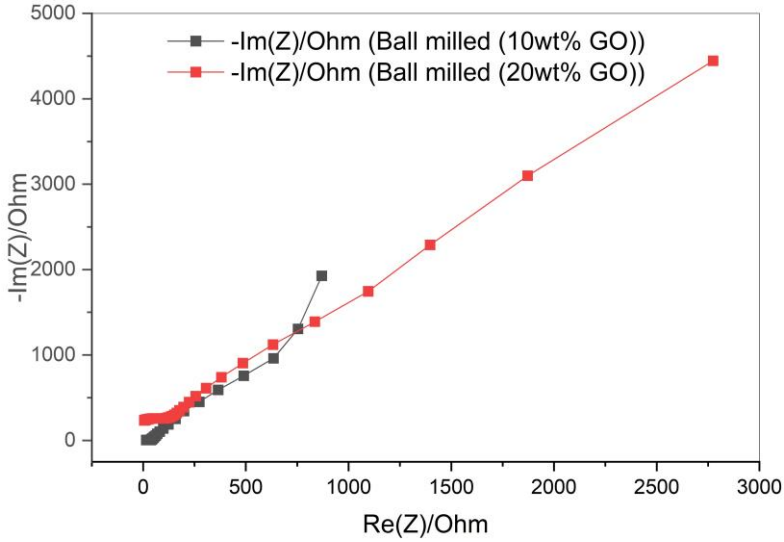

Figure 16 - EIS comparison of Silicon with 10wt% GO and 20 wt% GO

4.5.3 Cyclic Voltammetry (CV)

For both the coatings, Li was successfully alloyed with Si, as indicated from the peaks shown during electron transfer and discharge. However, 10wt% GO sample

demonstrated a sharper peak compared to 20wt% GO, which indicated more electrochemical activity - higher electrochemical performance. Although 20wt% GO sample provided a higher level of conductivity in comparison to the 10wt% GO and had a higher Li extraction and return to the electrode community. However, when compared against the 10wt% GO, 20wt% GO displayed broader peaks and lower intensities, thereby indicating less electrical connectivity and slower reaction kinetics. Additionally, when the 10wt% GO was compared to the 20wt% GO there is smaller Peak Separation denotes less polarisation between the two electrodes, hence a higher level of Lithium.

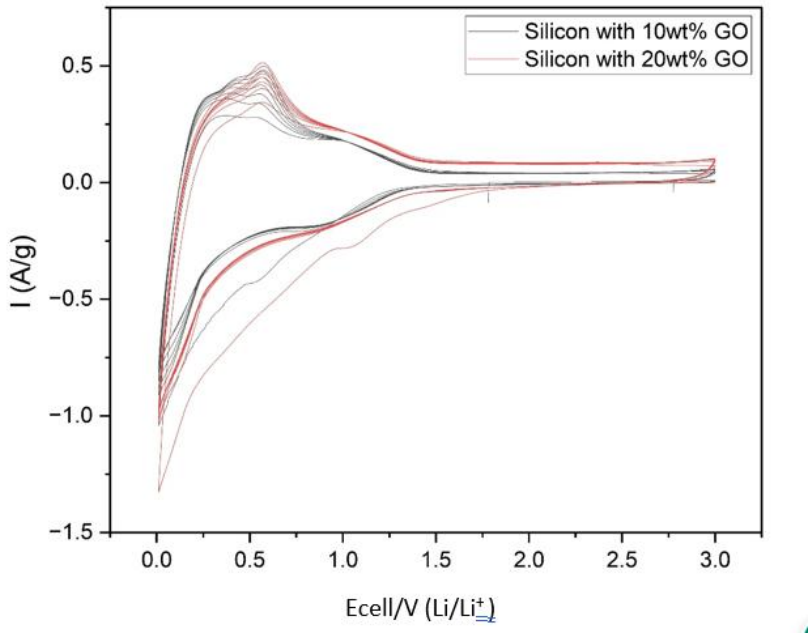

Figure 17 - Cyclic Voltammetry comparison of Silicon with 10wt% GO 20wt% GO

4.6 Comparative Cycle Performance of Different Coatings of Silicon and Graphene

- Silicon that was ball-milled and uniformly coated with graphene.
- Silicon that was ball-milled with GO (non-uniform coating).
- Silicon from commercial sources which is unmodified.
- Silicon that has been coated with a planetary mixer.

The current densities and voltage ranges used to cycle all four sample groups were identical.

In Initial Capacity Study, the capacity (discharge) of the ball-milled and uniformly coated sample has a significantly high initial discharge capacity (~3400 mAh g^{-1}). This indicates that this sample has a greater amount of active surface area available for

interfacial contact with the graphene coating, which in turn contributes to the improved performance. The commercial silicon and planetary-mixed silicon samples produced similar initial capacities (~3200 mAh g^{-1}), while the ball-milled silicon combined with GO shows only a slightly lower initial capacity (~3000 mAh g^{-1}).

Cycling capacity decay parameters a large difference is noted in the cycling performance of the four sample configurations after several cycles. The ball-milled silicon that has been uniformly coated with graphene maintains the greatest capacity retention (1600-1800 mAh g^{-1}) over a 25-cycle period. Commercial silicon starts out with a higher initial capacity, however within about ~15 cycles has lost most of it (>600 mAh g-1). The performance of the Si coated using a planetary mixer is similar to the commercial Si, but stabilizes at ~450-500 mAh g^{-1}, which indicates that the encapsulation of the silicon with the graphene is not very effective. Among the silicon samples that were coated, the ball-milled Si that has GO (not uniformly coated) degrades quicker than the others, falling below ~450 mAh g^{-1} after approximately ~20 cycles.

In summary the above testing indicates that the combination of ball-milling and uniform graphene coating produces the most stable and highest performance electrode configurations.Compared to the expected cycling performance of the uniformly coated and ball-milled Si, the comparative cycling data show that the benefits of particle size, coating uniformity and cycled processing on graphitic Si-type materials can be assessed from detailed mechanistic studies.

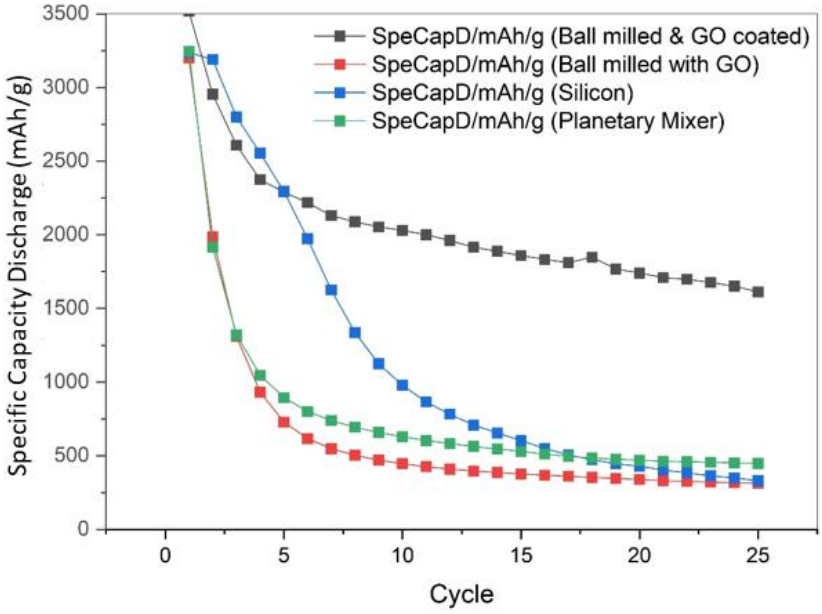

Figure 18 - Cycling performance comparison of different methods

4.7 Observed Limitations and Performance Bottlenecks

Overall, considering the operational improvements achieved through the modified coating processes, it was still evident at this advanced stage of work that there remained some limitations:

1. **Agglomeration of graphene at higher concentrations**

When applying higher concentrations of graphene material, instances of restacking and clustering were revealed, showing limited available surface area, increased mass of the electrode without any noticeable improvement in conductivity, or specifically energy related.

2. **Coverage still exposed Si**

When looking at the exposures of Si, evidence of centres of localized SEI were still produced and this in larger cycles, attributed to the increased impedance over longer cycling durations.

3. **Volume Expansion of Si**

Although there was an improvement with expanded Si and its effects limited significant particle size reduction, and was still partially broken down when looked into prolonged cycles. Although it provided variation to the conclusions, these observations and recollections added limited data on the overall lifetime.

4. **Process refinement with binder, slurry optimization**

After the drying process was completed, there have been electrodes where cracking was caused, thus indicating there was a need for process refinement in the binder system (e.g. changing ratios of CMC/SBR, or coming to alginate binders for elasticity purposes).

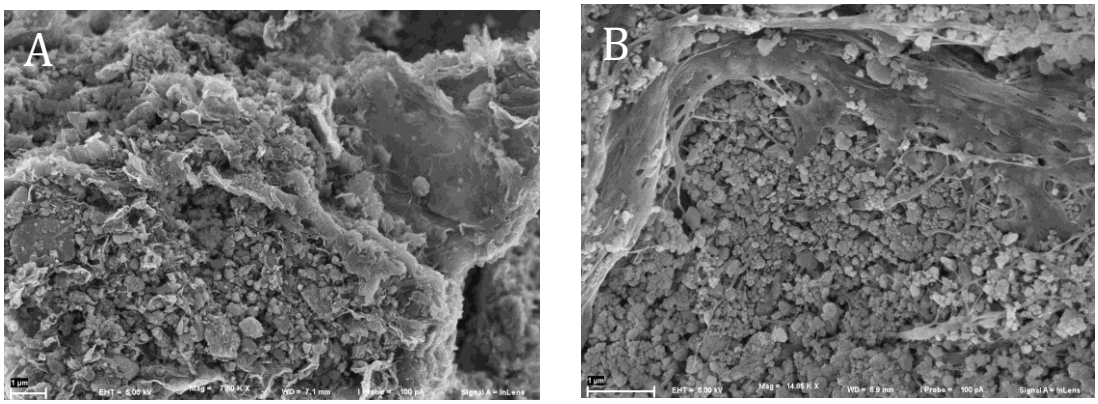

Figure 19 - SEM images of graphene agglomeration on silicon

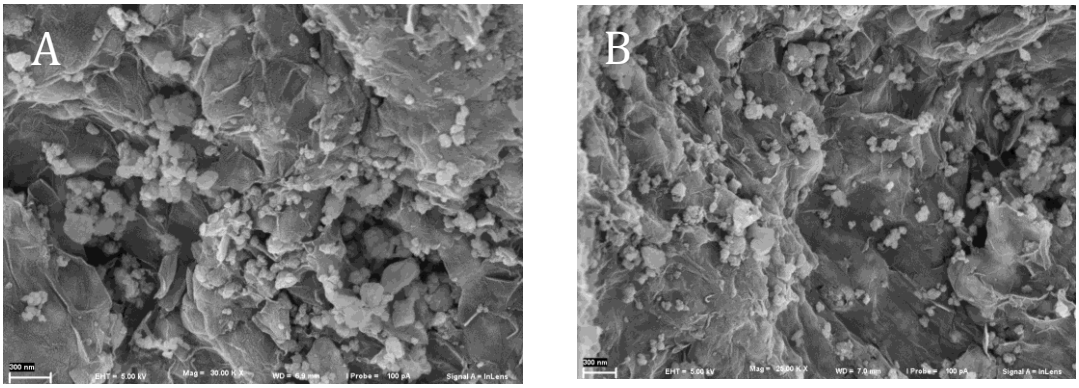

Figure 20 - Non-uniform graphene coating on SIlicon

Table 4 - Different aspects effect on bare silicon and their improvement after adding graphene.

Aspect	Effect on Silicon Anodes	Improvement by Graphene
SEI formation	Repeated cracking and reformation	Graphene limits direct electrolyte contact, forming uniform SEI
Coulombic efficiency	Low (~50–60%) due to lithium consumption	Increased to ~70–80% with graphene coatings
Charge-transfer resistance (R_ct)	Grows rapidly with cycling	Stabilized due to conductive graphene network
SEI composition	Organic-rich, unstable	Inorganic-rich (LiF, Li_2CO_3), mechanically robust
Cycle stability	Rapid capacity fading	High retention (>80% after 200 cycles)
Overall performance	Short life and poor reversibility	Long life, stable operation, low impedance

5 Discussion

The experimental results presented in the laboratory section of this study provide strong evidence that applying a graphene coating to micron sized silicon (Si) particles results in a marked improvement in the electrochemical performance of those anodes. This section links the results to essential fundamentals of lithium-ion storage, interfacial stability and charge transport to understand how the Si particle treatment, coating, and mixing improved the performance of the battery.

5.1 Effect of Particle Processing (Ball Milled and Commercial Si)

In this case, the characterization of the ground Si nanoparticle versus the commercial nanoparticle showed the substantial impact size and surface area can have on graphene adhesion and interfacial performance. The ball milled Si particles were smaller (~1-3 μm) but had a rougher surface area as shown in the SEM images (Fig-4), which contributed to a higher surface area for graphene adherence and more even distribution of the coating. The smaller size of the particles and irregular surface produced a stronger Si–O–C bond during APTES functionalization and subsequent GO coating resulting in a more dense conductive network of the Si particles. This is seen in the CV measurements of the ball milled Si-graphene in (Fig-5) which show sharper redox peaks. This indicates increased electronic conductivity and lithiation / delithiation kinetics for the ball milled Si Si-graphene compared to the commercial Si.

The enhanced cycling stability (Fig-6) approximately 70% capacity retained after 25 cycles – is likely related to better uniformity of the current distribution and greater ability to accommodate mechanical stress resulting from smaller particle size and improved coating coverage. It is indicating that reducing Si particle size increased cycle life and lowered interfacial resistance when combined with a conductive carbon matrix.

5.2 Effect of Graphene Coating on Ball-Milled Si

Results comparing the ball-milled Si with and without graphene coating suggest that the sample coated with graphene had superior performance for all electrochemical test considerations.

The cyclic voltammetry results from (Fig-9) show that between cycles, the uncoated Si electrode had broader and less defined peaks after several cycles, suggesting loss of active material connectivity and unstable growth of the solid electrolyte interface (SEI). For the graphene-coated Si sample, distinct and overlapping anodic and cathodic peaks were present over numerous cycles reflecting a reversible lithiation and delithiation process. The findings suggest that graphene improved electronic conductivity and retained a stable interface after cycling.

The cycling test data (Fig-9) demonstrated that the uncoated Si experienced rapid dissipation of capacity, retaining less than 50% of the original capacity after 100 cycles due to pulverization and repeated formation of a solid-electrolyte-interphase (SEI) layer. The graphene coated Si demonstrated an enhanced cycling stability; capacity retention was approximately 70% after 25 cycles, and the coloumbic efficiency remained above 99% after the initial few cycles. It is of note that this improvement to

capacity retention can be attributed to the mechanical flexibility and high conductivity of graphene, which effectively served a dual buffer role by both mechanically containing the volume expansion of Si, and by permitting electron transport.

5.3 Method Comparison (Planetary vs Conventional Mixing)

The method of coating was determined to be a significant determining factor on electrochemical stability and that uniformity of coating was contingent upon technique. In the planetary mixing method, the GO was susceptible to agglomeration due to the high shear and centrifugal forces, which resulted in incomplete coating (gaps in coating were visible). The mechanical de-agglomeration of the GO into the coating with planetary mixing resulted in current density hot spots which had caused rapid destruction of the SEI layer and additional impedance, which would have been considered to be a significant contributing factor to the unstable CV peak intensities. In contrast, the conventional mixing process yielded a homogeneous dispersion of graphene and an even coating layer, as depicted in (Fig-10). By adding APTES Si was further improved, hence enhancing the favorable electrostatic attraction with the negatively charged GO sheets. Consequently, this chemical interaction facilitated the transfer of electrons, resulting in stronger Si–O–C bonding of the graphene composition and conformal wrapping wrapped after reduction by hydrazine.

The improved uniformity of the graphene coverage resulted in the formation of the SEI primarily on the graphene surface and not as much directly on Si in a way that would cause excessive SEI growth.

5.4 The Influence of GO Loading on Morphology and Electrochemical Behavior

The SEM images that show the Differences in the morphology of silicon coated with 10 wt% vs. 20 wt% Graphene (Fig-13) demonstrate the significance of appropriate selection of the quantity of graphene needed to provide an effective structure for coating. When being coated with 10wt% GO, a coating exists that has dispersed sufficiently evenly to close in on the particle surfaces, hence creating an even conductive shell around silicon particles, thereby providing percolation of electrons throughout the silicon particles, providing efficient transfer of charged entities and providing adequate buffering capacity during the silicon volume expansion due to cycling. The structure of interconnected wrinkled graphene produced at this coating level is ideal for maintaining flexibility and mechanical integrity while in service.

However, when Si was coated with 20wt% GO, the coatings are beginning to aggregate. The additional GO sheets tend to restack, resulting in thicker and less uniform areas. Agglomeration results in decreased surface area, increased inactive mass, and may impede the diffusion of lithium cations. Furthermore, the dense restacked areas of GO are not able to flex uniformly in the event of silicon expansion therefore resulting in delamination or localised points of stress concentration during cycling.

These morphological differences observed directly influence electrochemical performance, therefore, the GO coating produced from the use of 20wt%GO will demonstrate increased Diffusion limitations, increased Impedance and decreased rate

capability due to the thickness of the coating and clustering. Reports have suggested that the optimal GO/Silicon ratio is usually between 5 to 15wt%, providing a balanced and good performance relative to conductivity and uniformity of coatings.

So although increasing GO content results in increased coverage, this does not equate to improved performance unless the GO remains uniformly dispersed. The SEM evidence attained indicates that a moderate loading of GO (10wt%) provides the basis for an acceptable coating in terms of coating properties (i.e. quality), conductivity, flexibility and interfacial stability.

5.4.1 The Graphene Content (Loading) of the Conductive Layer Impacts the Performance of the Silicon

Even through the 20wt% loading of GO provides a greater volume of Conductive Carbon, the findings indicate that they produced less long-term stability in cycling performance. The reason for this occurs because of the increased thicknesses (as seen in the SEM images) of larger Graphene sheets and not as much to the significant improvement in conductivity. Consistent with the added thickness of GO increases the mass of the electrodes while maintaining lower than proportional levels of conductivity increases. In essence, too much graphene restricts the amount of Li diffusion through the dense GR areas in addition to providing little mechanical compliance when compared to the layers of silicon in the direction of the thickness of the GR layer preventing it from as easily buffering the expansion of the Si.

On the other hand, the use of 10wt% GO creates a thin flexible GR layer, which remains in contact with both electrodes and retains most of the silicon's expansion, thereby providing a greater overall level of capacity retention than when a thicker GR layer has been used.

Based on the results of EIS, it is clear the following, the 10wt% GO sample provides very low charge transfer resistance and the 20wt% GO sample produced higher levels of charge transfer resistance (R.ct), therefore producing decreased electron transfers in cycles. The smaller amount of GR coverage on the 10wt% GO allows for a direct pathway for the electrons to travel from the silpriate layer to the collector layers. An excessive amount of GR will overload the direct pathways for the electrons and add an additional barrier, thus increasing the overall charge transfer resistance.

Additionally, sing the 10wt% GO coating allows for improved movement of Lithium Ions through the microstructure. On the other hand, the 20wt% GO creates a blocking effect to Li transport, confirming the results of increased impedance and steeper slope. Therefore, when comparing the EIS results to the cycling data, they correlate: a better-interfaced electrochemical stability and a higher level of interfacial homogeneity, were produced, initially with the use of 10wt% GO. Continued use of excessive GO creates greater resistance losses and ultimately limits the lithiation kinetics.

5.5 Particle Size and Surface Activation Influence on different coating methods

The cycling performance of ball-milled Si is significantly improved when compared to the cycling performance of as-received commercial Si. This performance improvement is primarily attributed to the fact that:

Reduced particle size provides for a decrease in internal stress associated with lithiation excess surface area improves graphene's hosting and adhesion to Si's SurfaceActivation of surface chemistry on Si provides for stronger covalent bonds between graphene and Silicon. These characteristics of ball-milled and uniformly coated Si provide the basis for the outstanding performance of ball-milled Si prior to even considering the influence of coating on the overall cycling performance.

5.5.1 Coating Uniformity

Uniformly coated Si has the highest cyclical performance of all of the mixtures demonstrating that in order for graphene to exert its synergy on Si, a continuous conformal and electrically conducting coating is required on Si particles to allow:

- Buffering (<300% expansion) of the volume expansion of Si mantaining the integrity of electronic conduction pathways.
- Preventing multiple cracking and reforming of the SEI; Reducing charge-transfer resistance

In other words, the coating methodology used to apply the graphene is of equal importance as the content of the graphene coating in predicting the performance of the resulting graphitized Si material.

5.5.2 The Effects of Planetary-Mixing and Poor Performance

Planetary mixing induces substantial shear forcing the agglomeration of GO Sheets of Graphene and the clustering of GO Sheets into thick stacks, resulting in the failure of GO Sheets to achieve adherence to the surface of the Si. This results in increased impedance, instability in the formation of the SEI, and decreased retention of cycling capability.

Table – 5 Comprative study of different methods of graphene coating on SIlicon.

Sample Type	Initial Capacity (mAh g^{-1})	Capacity @ Cycle 10 (mAh g^{-1})	Capacity @ Cycle 25 (mAh g^{-1})	Overall Trend
Ball-milled & uniformly graphene-coated Si	~3400	~2100	1600–1800	Highest stability, gradual fading, best retention
Ball-milled Si mixed with GO (non-uniform)	~3000	~900	400–500	Fast fading due to coating defects and high impedance
Commercial silicon (uncoated)	~3200	~1100	450–500	Rapid degradation due to particle cracking & unstable SEI
Planetary mixer GO-coated Si	~3200	~1200	450–500	Poor GO dispersion causes similar fading as uncoated Si

6 Conclusions

The research in this thesis has focused on developing and assessing an appropriate graphene-based coating method for commercial micron-sized silicon particles, specifically highlighting coating uniformity, interfacial interactions, and the procedure's scalability. By methodically improving material processing parameters and slurry formulation, insights were obtained concerning the impact of surface chemistry and particle size on the stability and consistency of electrode fabrication. The results enhance comprehension of the mechanisms by which acid-assisted graphene coating and ball-milling augment the electrochemical stability of silicon anodes. SEM images confirm the production of a uniform, wrinkled graphene layer that adhered to the Si surface, whereas planetary mixing produced a non-uniform coating with poorer adhesion. Graphene was better dispersed due to enhanced protonation of the amine-functionalized Si (APTES-modified) surface, enabling stronger electrostatic interactions, more uniform adsorption of graphene oxide (GO) sheets, and their redistribution. Ball-milled Si had superior coating adhesion and overall interfacial contact, due to its smaller particle size, which increased surface area.

In Cyclic Voltammetry the graphene-coated Si electrodes showed sharper, more symmetric, and overlapping redox peaks; indicative of reversible lithiation/delithiation and diminished polarization in relation to the uncoated Si and EIS Results showed the charge-transfer resistance (R_ct) was ~100–120 Ω for the graphene-coated electrodes as compared to ~400–450 Ω for the bare Si, indicating improved electronic conductivity and enhanced inter-facial stability. The GCD of the coated electrodes indicated better first cycle coulombic efficiency (~70%) and stable voltage plateaus at about ~0.1 V, showing moderated SEI formation and cycling stability after 25 cycles of cycling, the graphene-coated Si electrodes could retain ~70% of their initial capacity (~800 mAh g^{-1}) whereas the bare Si retained less than 40%. The low-rate capacity (~75%-80%) at 1C was maintained with the coated electrodes, showing very good kinetics and lithium diffusion capabilities. The graphene coating acted as a mechanical buffer, minimizing Si expansion (~300%), preventing crack formation, and maintaining electrical continuity. Graphene also served as a conductive scaffold, enabling uniform current distribution and minimizing local overpotentials. The acid-assisted graphene/ball-milled Si coating provided strong interfacial Si–O–C bonding, improving charge-transfer kinetics and long-term performance stability. Additionally, the coated graphene layer acted as a mechanical buffer, reducing the ~300% volume expansion of Si and preventing cracking that would have disrupted electrical connectivity. It performed a conducting function that promoted homogenous current distribution and limited localized overpotentials. The chemical stability of graphene allowed the SEI to form primarily on the graphene surface, leading to a thin, stable, inorganic-rich SEI (LiF, Li_2CO_3) as evidenced by consistent impedance behaviour across cycling. Acid-assisted coating of graphene produced strong interfacial Si–O–C bonding, facilitating charge transfer and enhancing stability during long-term cycling. The acid-assisted ball-milled Si-graphene-optimized composite exhibited enhanced electrochemical performance compared to both commercial Si and planetary-coated samples across all metrics. The capacity retention (~70%) with first cycle efficiency (~70%) and R_ct (<120 Ω) were comparable to or better than those reported in literature with micron-Si–graphene systems. Most importantly, the developed process is cost-effective, reproducible, and scalable to an industry-level for commercially available micron-Si powders, compared with the expensive nanosilicon or hybrid oxide structure alternatives.

7 Future Scope

7.1 Coating optimization

Direct the loading of graphene and coating thickness through fundamental process parameter optimization (e.g., concentration of GO, strength of acid, mixing time) that balances the conductivity of the coating with its available active matter, and thus improve potential capacity retention for high-energy-density devices. Evaluate spray-drying or fluidized-bed coating techniques to develop scalable production of uniform coating at the gram to kilogram level.

7.2 Electrolyte engineering

Test new functionalized electrolytes (e.g., fluoroethylene carbonate (FEC), LiDFOB) which can form a more thermodynamically favored inorganic SEI layer on the Si and graphene anodes. The interactions between the electrolyte additives and the graphene-coated graphite anodes will be evaluated to minimize solvent co-intercalation and minimize gas generation during oxidation. Temperature variation in the cycling behaviour of the fully deposited Si anodes is critical to monitor as stable SEI and coating remain at elevated operating temperatures (≥60 °C).

7.3 Binder and slurries

Consider using alternative elastic self-healing polymeric binders (e.g., PAA, or PAA-CMC blends) rather than conventional PVDF or CMC binders to accommodate the Si volume changes. Examine the impact of slurry rheology and the solids-content for electrodes to evaluate their mechanical reliability and porosity as a function of high areal capacity.

7.4 Full-cell tests and cycle tests

Pair the optimized anodes with high voltage cathodes for full-cell test appraisals (e.g., NMC811 and LFP cathodes) to assess performance scalability and energy density improvements. Long term cycling (>500 cycles) will determine the mechanical stability, ability for electrolyte to infiltrate, and coulombic efficiencies at practical loading. Post-mortem data will need to be collected for extended cycling performance for failure classification (e.g., particle cracking, binder pull-off, and SEI thickening).

7.5 Sustainability and scalability assessment

After evaluation of component and design feasibility an economic and life cycle analysis (LCA) will need to be conducted to evaluate the agreement between performance when comparing graphene-coated Si vs. graphite and aspect of energy consumption, and any carbon or environmental consequences that may arise.
Alternative environmentally sustainable synthesis possibilities for the coated graphene should also be studied (e.g., biomass derived graphene, or reduction alternatives).

8 References

1. A comprehensive review of silicon anodes for high-energy batteries. . Feyzi, E., et al. s.l. : Journal of Energy Storage., 2024.

2. Innovative solutions for high-performance silicon anodes. . Khan, M., et al. s.l. : Renewable and Sustainable Energy Reviews., 2024.

3. Tailoring SEI composition for mechanically reinforced silicon anodes. . Tian, Y. F., et al. s.l. : Nature Communications, 2023.

4. Effect of graphene on the performance of silicon–carbon composite anode materials. Ni, C., Xia, C., Liu, W., et al. 2024.

5. Functional graphene coatings in electrochemical energy storage systems. . Qu, Q., et al. s.l. : Electrochimica Acta., 2025.

6. Wrinkled multilayer graphene for high-areal-capacity silicon anodes. . Kang, M. S., et al. s.l. : Advanced Energy Materials, 2022.

7. Micron-sized silicon–graphite–carbon composites with enhanced stability. Zhao, F., et al. s.l. : Electrochimica Acta., 2022.

8. Innovative solutions for high-performance silicon anodes. . Khan, M., et al. Renewable and Sustainable Energy Reviews., 2024.

9. Reduced graphene oxide-encaged submicron-silicon anodes with hybrid Al_2O_3/rGO shells for stable cycling. . Tan, X., et al. s.l. : ACS Applied Energy Materials., 2024.

10. Coal-derived graphene foam hosting micron-sized silicon for high-performance lithium-ion batteries. Zhang, X., et al. 2022.

11. Obrovac, M.N. and Christensen, L. Structural changes in silicon anodes during lithium insertion/extraction. s.l. : Electrochemical and Solid-State Letters, 2004.

12. Coal-derived graphene foam and micron-sized silicon composites for high-performance LIBs. Zhang, X., et al. 2022.

13. Dual carbon encapsulated porous micron silicon (P-Si-rGO-C) composites for LIBs. Journal of Colloid and Interface Science. Shi, H., et al. s.l. : Journal of Colloid and Interface Science, 2024.

14. Dual carbon encapsulated porous silicon composites for lithium-ion battery anodes. Shi, H., et al. s.l. : Journal of Colloid and Interface Science, 2024.

15. Reduced graphene oxide-encaged submicron-silicon composites. . Tan, X., et al. s.l. : ACS Applied Energy Materials, 2024.

16. Barsukov, V. Electrochemical impedance spectroscopy in battery materials characterization. s.l. : Electrochimica Acta, 2022.

17. Dual carbon encapsulated porous micron silicon (P-Si-rGO-C) composites for LIBs. Shi, H., et al. s.l. : Journal of Colloid and Interface Science., 2024.

18. McDowell, M.T., Lee, S.W., Nix, W.D. and Cui, Y. In situ TEM of two-phase lithiation of amorphous silicon nanospheres. s.l. : Nano Letters, 2013.

19. Ryu, I., Choi, J.W., Cui, Y. and Nix, W.D. Size-dependent fracture of silicon nanoparticles during lithiation. . s.l. : Journal of the Mechanics and Physics of Solids, 2011.

20. Hatchard, T.D. and Dahn, J.R. In situ XRD and electrochemical study of the reaction of lithium with amorphous silicon. . s.l. : Journal of the Electrochemical Society, 2004.

21. Beaulieu, L.Y., Eberman, K.W., Turner, R.L., Krause, L.J. and Dahn, J.R. Colossal reversible volume changes in lithium alloys. . s.l. : Electrochemical and Solid-State Letters, 2001.

22. Zhao, K., Pharr, M., Vlassak, J.J. and Suo, Z. Fracture of electrodes in lithium-ion batteries caused by fast charging. s.l. : Journal of Applied Physics, 2010.

23. Functional graphene coatings in electrochemical energy storage systems. Qu, Q., et al. s.l. : Electrochimica Acta., 2025.

24. Tailoring SEI composition for mechanically reinforced silicon anodes. Tian, Y. F., et al. s.l. : Nature Communications, 2023.

25. Coal-derived graphene foam and micron-sized silicon composites for high-performance LIBs. Zhang, X., et al. 2022.

26. Wrinkled multilayer graphene for high-areal-capacity silicon anodes. . Kang, M. S., et al. s.l. : Advanced Energy Materials., 2022.

27. Reduced graphene oxide-encaged submicron-silicon composites. . Tan, X., et al. s.l. : ACS Applied Energy Materials, 2024.

28. The electrochemical behavior of alkali and alkaline earth metals in nonaqueous battery systems—The solid electrolyte interphase model. . Peled, E. s.l. : Journal of the Electrochemical Society, 1979.

29. Electrolyte and interphase chemistry in high-energy lithium batteries. . Xu, K., et al. s.l. : Chemical Reviews, 2021.

30. Effect of graphene on the performance and SEI evolution of silicon–carbon composite anode materials. Ni, C., et al. 2024.

31. Cyclic voltammetry analysis of silicon–graphene composites in lithium-ion batteries. Xie, J., et al. s.l. : Electrochimica Acta, 2023.

32. Effect of graphene on the performance of silicon–carbon composite anode materials. Ni, C., Xia, C., Liu, W., et al. 2024.

33. Tailoring SEI composition for mechanically reinforced silicon anodes. . Tian, Y. F., et al. s.l. : Nature Communications, 2023.

34. Micron-sized silicon–graphite–carbon composites with enhanced stability. . Zhao, F., et al. s.l. : Electrochimica Acta., 2022.

35. A comprehensive review of silicon anodes for high-energy batteries. et.al, Feyzi. E. s.l. : Journal of Energy Storage., 2024.

36. Structural changes in silicon anodes during lithium insertion/extraction. Obrovac, M.N. and Christensen, L. s.l. : Electrochemical and Solid-State Letters, 2004.

37. Size-dependent fracture of silicon nanoparticles during lithiation. . Liu, X.H., Zheng, H., Zhong, L., et al. s.l. : ACS Nano, 2012.

38. In situ TEM of two-phase lithiation of amorphous silicon nanospheres. . McDowell, M.T., Lee, S.W., Nix, W.D. and Cui, Y. s.l. : Nano Letters, 2013.

39. A review of the electrochemical performance of alloy anodes for lithium-ion batteries. Zhang, W.J. s.l. : Journal of Power Source, 2011.

40. Interconnected silicon hollow nanospheres for lithium-ion battery anodes. Yao, Y., McDowell, M.T., Ryu, I., et al. s.l. : Advanced Materials, 2011.

DEPARTMENT OF SUSTAINABLE ENERGY SYSTEMS
CHALMERS UNIVERSITY OF TECHNOLOGY
Gothenburg, Sweden 2026
www.chalmers.se

CHALMERS
UNIVERSITY OF TECHNOLOGY